

Design of efficient LCC based on ICL5102/HV combo controller IC

Focusing on applications with wide output voltage and current range

Author: Dr. Yi Wang – Principal Product Definition Engineer

About this document

Scope and purpose

In many power supply applications, the load can have a wide operating range, in terms of both voltage and current. LED lighting and battery charging applications are typical examples. The LLC topology is normally a popular choice thanks to its intrinsic high efficiency and user-friendly fundamental harmonics analysis (FHA) design approach. However, it also has shortcomings, such as limited voltage operating range when the load current range goes wide. Additionally, although the FHA approach is quite accurate around the series resonant working point, this does not remain valid as the load range (both voltage and current) significantly widens.

Here, LCC, as another load-resonant topology, can be an attractive alternative for wide-load operation. However, design of LCC topology is not as straightforward as LLC because it seldom works around its series resonant point, where the entire circuit can be linearized. Therefore, the FHA approach generates unacceptable inaccuracy, which results in much design time and effort being spent for iterative optimization of the resonant tank.

This article will first compare LLC and LCC in a qualitative way, and explain why LCC is a better choice for applications with wide operating range. Second, design guidelines for an efficient LCC are given. To facilitate an easy, fast and accurate LCC design, a time-domain-based design tool has been developed, and its use will also be described.

This LCC design tool is specially developed for ICL5102, a combo controller for boost PFC + resonant half-bridge (HB) topology such as LLC and LCC. It can be broadly used for LED lighting and other power supplies where the system bill of materials (BOM) cost, input power quality, power density, standby power and product reliability are critical design indices. Based on ICL5102, several interesting reference boards have been designed for (but not limited to) LED lighting applications, to demonstrate the unique values that ICL5102 can deliver to our customers. These reference boards include:

- a 100 W high-frequency LCC (180 kHz~450 kHz)
- a 52 W open-loop controlled LCC with narrow output current spread, and
- a 150 W high-voltage (HV) LCC (800 V input) board

Apart from the open-loop controlled LCC, which is a non-dimmable on/off LED driver, the rest can all dim down to 1 percent of the full load in a wide LED voltage range.

Intended audience

This document is intended for technical experts and power supply designers who intend to use ICL5102 for an efficient LCC design of a power supply with a wide operating range.

Table of contents

About this document.....	1
1 Introduction	4
1.1 Applications with wide operating range.....	4
1.2 Introduction to ICL5102.....	5
1.2.1 Key features.....	5
1.2.2 Protection coverage.....	5
2 LLC vs. LCC	7
2.1 Fundamental harmonics analysis.....	7
2.2 Topology comparisons.....	9
2.2.1 Soft-switching range	9
2.2.2 Consequence of load faults	10
2.2.3 Voltage gain range and frequency span.....	10
2.2.4 Voltage source vs. current source.....	11
2.2.5 Sensitivity to the parasitic capacitance	12
2.2.6 Integrated transformer structure	13
2.2.7 Light-load loss.....	14
2.3 Summary.....	14
3 LCC operation and design guidelines	15
3.1 Operation modes.....	15
3.1.1 High-power mode	15
3.1.2 Low-power mode	16
3.1.3 Zero-power mode	17
3.2 A practical design rule for an efficient LCC converter	18
3.2.1 Efficiency indicator of an LCC converter	18
3.2.2 A practical design rule for high efficiency at full load	19
4 Design tool for LCC with wide load range	21
4.1 Working principle	21
4.2 Assumption, input and output of this tool	22
4.2.1 Assumption.....	22
4.2.2 Input and output	22
4.3 Design charts	23
4.3.1 RMS/AVG chart.....	23
4.3.2 L_s chart.....	24
4.3.3 Extraction of optimal parameters	25
4.4 Result validation.....	28
4.5 Summary.....	29

Table of contents

5	LCC design examples based on ICL5102	30
5.1	Frequency set circuit of ICL5102	30
5.1.1	Frequency set in the steady-state	30
5.1.2	Frequency behavior in the start-up process	32
5.2	A high-frequency LCC design example – 100 W	33
5.2.1	System specification and LCC design inputs	34
5.2.2	Design and performance.....	34
5.3	A low-cost open-loop controlled LCC design – 52 W	36
5.3.1	System specification and LCC design inputs	36
5.3.2	Design and performance.....	37
5.4	HV LCC – 150 W.....	42
5.4.1	System specification and performance	42
5.4.2	Design and performance.....	43
5.5	Summary.....	44
6	References	46
	Revision history.....	47

Introduction

1 Introduction

This chapter reviews the typical power supply applications where the wide operating range is required, and introduces the features of ICL5102 that can control and drive the LLC and LCC topology following a PFC converter.

1.1 Applications with wide operating range

In many power supply applications, a load with a very wide operating range is necessary. Mid- and high-power LED window drivers and Li-ion battery chargers are typical examples.

LED lighting: **Figure 1** shows a typical output operating window of an outdoor LED driver. It can be seen that the LED load voltage that this driver feeds is 100 V~300 V. The voltage ratio, which is the ratio between maximum and minimum voltage, is three times, while the LED should be able to dim down to less than 10 percent of the maximum current. In an indoor lighting application, it can dim down to 1 percent. Additionally, in some mid-range and high-end LED drivers, there is a nearly constant power range crossing a certain LED voltage range, e.g., between 300 V and 220 V in **Figure 1**. This makes the LED driver design more challenging.

Battery charger: **Figure 2** illustrates a typical charging profile of the Li-Ion battery used in an e-bike charger. Normally three charging phases are present: the precharging phase when the battery is deeply drained, the constant current (CC) phase when the battery voltage rises above a certain level, and the constant voltage (CV) phase in which the battery voltage stays constant but the current drops gradually as the battery is nearly fully charged. In this process the battery voltage increases to more than two times its lowest value, and the charging current rises eight times from its minimum. Therefore, both applications require a power supply that can handle this wide operation range, preferably with high efficiency at limited cost.

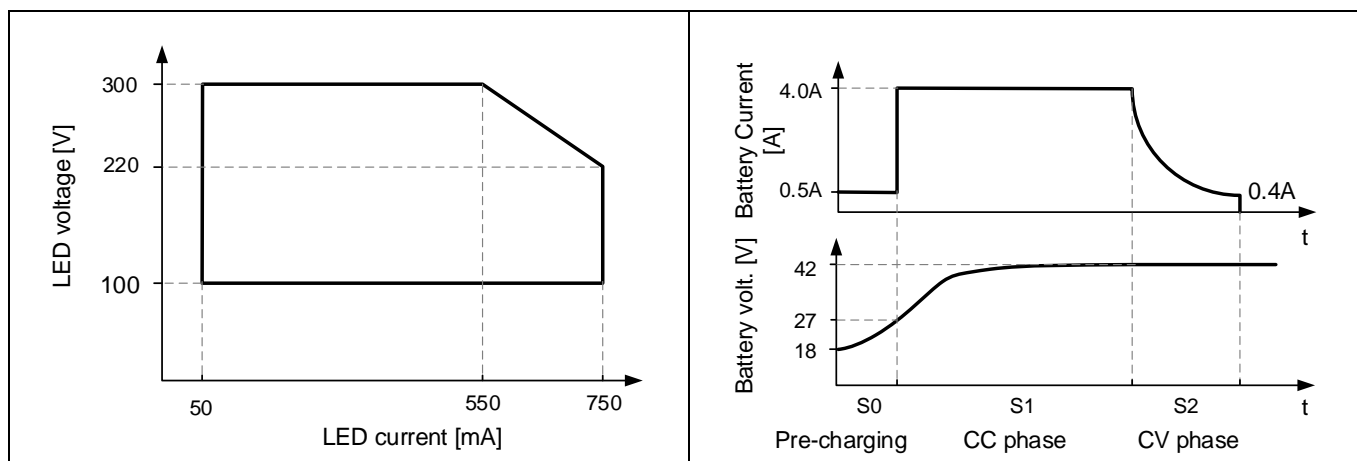


Figure 1 Typical output operating window of an outdoor LED driver

Figure 2 Typical Li-ion battery charging profile of an e-bike application

Generally, for DC-DC power conversion above 75 W, the LLC converter is popular in these applications due to the good efficiency from its soft-switching capability and the efficient power transfer pattern. Meanwhile LCC, also a member of the load-resonant converter family, does not attract much attention in the industry. One important reason could be that there is no proper analysis tool available on the market. The following chapters will highlight the unique properties of LCC that make it an attractive topology for the wide-operating power supply, and more importantly, propose and explain our easy, accurate and non-iterative tool for LCC design.

Introduction

1.2 Introduction to ICL5102

ICL5102 is an integrated combo IC designed to drive and control the boost PFC + resonant HB topology (LLC or LCC) in combination. The normal voltage version (650 V max.) can cover the applications with universal mains up to 305 V_{RMS} from the HB driver point of view, while its HV version, ICL5102HV, can handle 980 V (max. value), which fits horticultural lighting applications and other industrial applications where the input mains voltage is up to 530 V_{RMS}.

The pin maps of ICL5102 and ICL5102HV are given in **Figure 3**. Thanks to Infineon's proprietary coreless transformer technology, ICL5102/HV's high-side MOSFET driver is very robust against dV/dt and negative voltage peak on the switch node of the HB, and it is very efficient at high operating frequency.

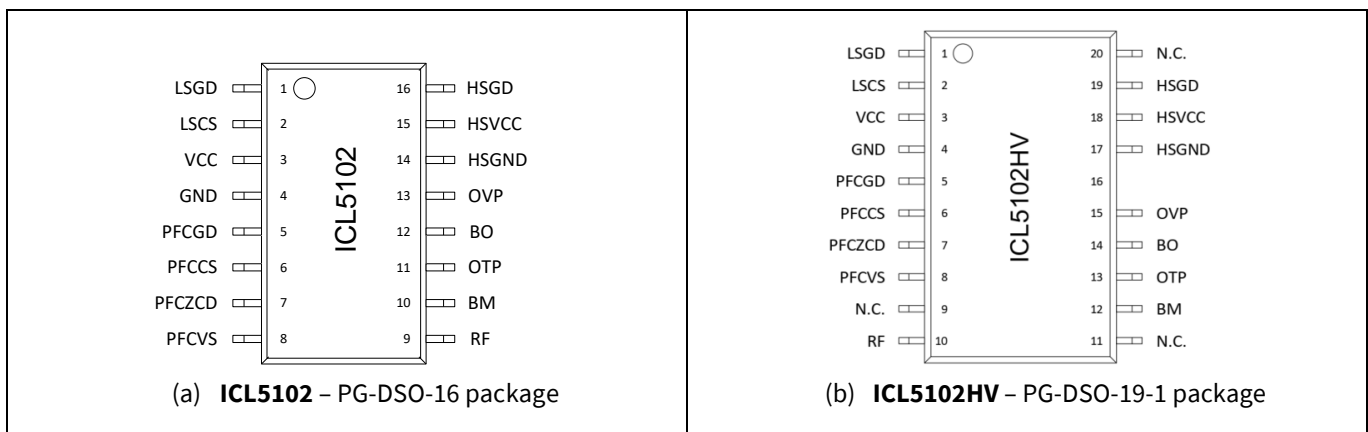


Figure 3 Pin maps of (a) ICL5102 and (b) ICL5102HV

The other key features and the protection coverage are summarized as follows:

1.2.1 Key features

- Maximum **500 kHz** HB switching frequency in continuous operation and at extreme temperatures, which enables a high-power-density LLC/LCC design.
- The HSGND pin, connected to the switch node of the HB, can handle huge negative voltage peak.
- HB frequency up to 1.3 MHz at soft-start.
- Adaptive dead time.
- A proprietary phase feed-forward control speeds up the dynamic response of the LLC/LCC converter, enabling a smaller output capacitor in CV applications.
- THD optimization ensuring best-in-class THD performance and low harmonic distortion at light load, helping the design pass IEC61000-3-2 class C edition 5.1. Please refer to our 130 W LLC engineering report [\[8\]](#) to see the excellent power-quality performance ICL5102 can achieve.
- PFC controller with critical conduction mode (CrCM) and discontinuous conduction mode (DCM) for the best efficiency in a wide load range.
- Resonant HB controller with fixed or variable switching frequency control.
- Burst mode supporting standby mode with low power consumption (less than 500 mW, system level).

1.2.2 Protection coverage

- Input brown-out protection
- PFC bus overvoltage protection (OVP)
- PFC overcurrent protection (OCP)

Introduction

- Output OCP/overpower protection (OPP)
- Output OVP protection possible
- HB capacitive mode protection
- Overtemperature protection (OTP)

2 LLC vs. LCC

This chapter will describe and compare the properties of LLC and LCC topologies, with emphasis on how widely they can operate in terms of voltage and current. The assumption here is that a PFC controlling the input voltage constant is available and the voltage ripple is negligible compared with the average input value.

2.1 Fundamental harmonics analysis

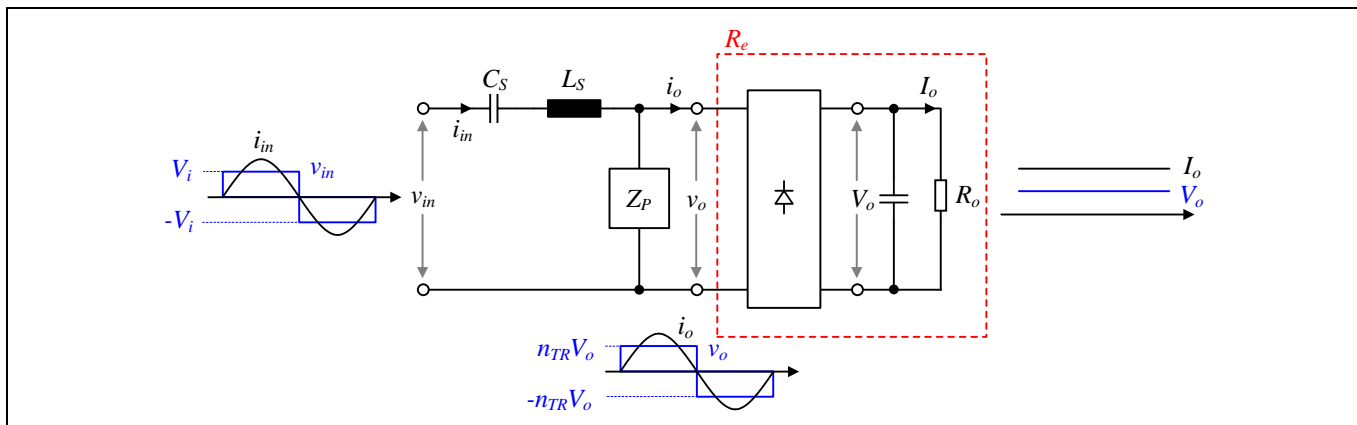


Figure 4 LLC/LCC circuit at the series resonance point (referred to the primary side)

The most popular approach to analyzing load-resonant converters (like LLC and LCC) is based on the FHA [1]. It assumes the circuit operates around the point that only the fundamental harmonic delivers power to the output. This assumption is valid when, for example, the LLC/LCC converter operates in the vicinity of its series resonant frequency f_R , which is formed by the series resonant capacitance C_S and series resonant inductance L_S (see Figure 4). Here, V_i is half of the bus voltage in the case of HB topology and equal to the bus voltage in the case of full-bridge (FB) topology. At f_R , the input current i_{in} is sinusoidal and in phase with the input voltage of square wave v_{in} . The voltage v_o across the parallel resonant impedance Z_P is also a square, and the current i_o flowing into the output rectifier is also sinusoidal and also in phase with v_o . Depending on whether it is LLC or LCC topology, the impedance Z_P is either an inductor L_P or C_P , respectively. Here, the isolated transformer is neglected and hence, every component on the secondary side is referred to the primary side. Notably, the output diodes are conducting continuously at this working point if the dead time required for the HB zero voltage switching (ZVS) is neglected. In a summary, the prerequisites of an accurate FHA are:

- a sinusoidal input current to the resonant tank that is in phase with the input square voltage
- continuous conduction of the output diodes.

Although this approach has limited accuracy when the operating points are far away from \mathbf{f}_R , which occurs as the load range widens, it can still be used to qualitatively describe the LLC or LCC for a quick and direct understanding of the topology's characteristics.

Under the assumption of FHA, the LLC/LCC circuit can be linearized and the load is equivalent to be a resistor R_e in parallel with Z_p . This equivalent circuit is given in **Figure 5**. Because only the fundamental harmonic delivers power to the output, the circuit can be analyzed with an AC signal. The load resistance R_o can be referred to the primary side to a value R_e , which generates the same power as the real load R_o . Its value is calculated as: [1]

$$R_e = \frac{8}{\pi^2} R_o n_{TR}^2 \quad \text{Eq. 1}$$

Where n_{TR} is the transformer turns ratio from the primary side to the secondary side. This equivalent AC circuit is given in **Figure 5**.

LLC vs. LCC

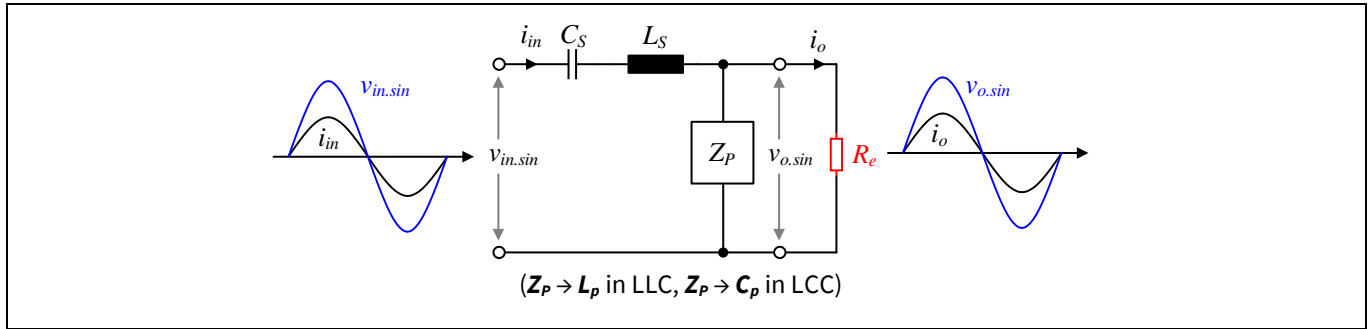


Figure 5 Linearized circuit of (a) LLC and (b) LCC in an FHA approach – at the series resonance point

Because the input and output are both converted from square waves to pure sinusoidal signals, the DC voltage gain $G_{V,DC}$ from input to output is equal to the AC voltage gain, and it can be calculated as:

$$G_{V,DC} = \frac{v_{o.sin}}{v_{in.sin}} = \left| \frac{Z_p}{Z(C_S) + Z(L_S) + Z_p} \right| \quad \text{Eq. 2}$$

Note that the $v_{o.sin}$ has to be lagging $v_{in.sin}$ in order to obtain the ZVS of the MOSFET. The G_V values for LLC and LCC are both given in [Table 1](#). The nominalized load current in R_e is defined as

$$J_{Norm} = \frac{G_{V,DC} V_I}{R_e} \bigg/ \frac{V_I}{\sqrt{\frac{L_S}{C_S}}} \quad \text{Eq. 3}$$

where $\sqrt{L_S/C_S}$ is the characteristic impedance Z_e of the series resonant elements and V_I is half bus voltage ($V_{BUS}/2$).

The key terms used to define the DC voltage gain are given in [Table 1](#).

Table 1 Definition of key terms in the FHA of LLC/LCC topology

Definition	LLC topology	LCC topology
R_e Equivalent load R_o is the real load resistance		$\frac{8}{\pi^2} R_o n_{TR}^2$
Q_e Quality factor		$\frac{1}{R_e} \sqrt{\frac{L_S}{C_S}}$
f_{RL} Lower resonant frequency	$\frac{1}{2\pi} \sqrt{\frac{1}{C_S(L_S + L_p)}}$	$\frac{1}{2\pi} \sqrt{\frac{1}{L_S C_S}}$
f_{RH} Higher resonant frequency	$\frac{1}{2\pi} \sqrt{\frac{1}{L_S C_S}}$	$\frac{1}{2\pi} \sqrt{\frac{C_S + C_p}{L_S C_S C_p}}$
f_n Normalized switching frequency	$\frac{f_{sw}}{f_{RH}}$	$\frac{f_{sw}}{f_{RL}}$
$f_{HL} (=f_{RH}/f_{RL})$ Resonant frequency ratio	$\sqrt{1 + \frac{L_p}{L_S}}$	$\sqrt{1 + \frac{C_S}{C_p}}$

LLC vs. LCC

Definition	LLC topology	LCC topology
$G_{V,DC}$ Voltage gain ($n_{TR}V_O/V_{in}$)	$\left \frac{(f_{HL}^2 - 1)f_n^2}{(f_{HL}^2 f_n^2 - 1) + j \cdot f_n Q_e (f_n^2 - 1)(f_{HL}^2 - 1)} \right $	$\left \frac{1}{\frac{f_{HL}^2 - f_n^2}{f_{HL}^2 - 1} + j \frac{Q_e}{f_n} (f_n^2 - 1)} \right $
J_{Norm} Normalized load current	$\left \frac{Q_e (f_{HL}^2 - 1)f_n^2}{(f_{HL}^2 f_n^2 - 1) + j \cdot f_n Q_e (f_n^2 - 1)(f_{HL}^2 - 1)} \right $	$\left \frac{Q_e}{\frac{f_{HL}^2 - f_n^2}{f_{HL}^2 - 1} + j \frac{Q_e}{f_n} (f_n^2 - 1)} \right $

The voltage gain and normalized load current are described in terms of the quality factor Q_e , the frequency ratio between two resonant frequencies f_{HL} and the normalized switching frequency f_n . Different from the FHA approach, which uses the ratio between two resonance inductances for the LLC case, using the f_{HL} term can help us understand the voltage gain scan curve more easily. The next chapter will explain LLC and LCC converters based on the FHA approach.

2.2 Topology comparisons

This section explains the essential differences between LLC and LCC converters, using the FHA approach described above. It covers the operating range, reaction to load faults, voltage gain, source type, sensivity to parasitics and etc.

2.2.1 Soft-switching range

Both LLC and LCC can operate with soft switching – namely, ZVS of the primary-side MOSFET and ZCS of the output diodes. **Figure 6** shows the voltage gain curves of both topologies in terms of switching frequency (x-axis) and different Q_e or R_e (curves). Here, the Z_e value is the same for all curves, and the curves of the same color in both figures have the same R_e value. The outer curve of the contour is the lower Q_e , and higher R_e are, in other words, smaller load powers.

When working in the inductive region (light green area) where the load current i_o falls behind v_{in} (see **Figure 4**), LLC and LCC achieve soft-switching, and hence high efficiency, reliability and good EMI performance.

There are two parts of the soft-switching area of LLC: one is below the LLC series resonant frequency $f_{RH,LLC}$ and the other above it. It is interesting to see from the green area above $f_{RH,LLC}$ that when the R_e goes high, the gain curve does not obviously drop, even as the frequency greatly increases. Therefore, it is not recommended to operate in this area when the specified load current range is really wide. There is another important reason for this, and it will be explained in **section 2.2.5**. Meanwhile, this is not the case for LCC in the soft-switching area. This is because as the frequency rises, the voltage across the LCC parallel resonant capacitor C_p fades away quickly, so the load current drops rapidly.

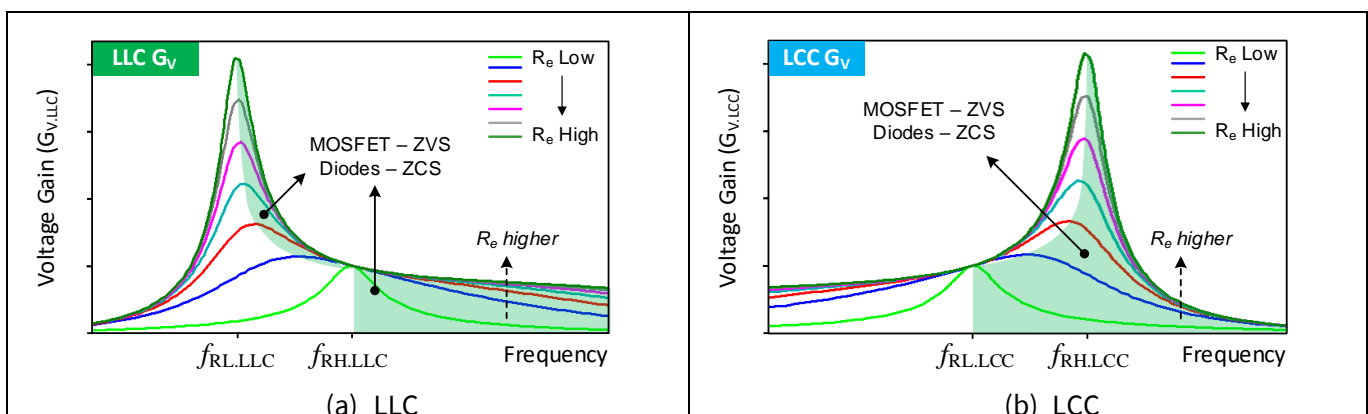


Figure 6 Soft-switching range in the voltage gain curves of LLC and LCC

LLC vs. LCC

2.2.2 Consequence of load faults

Let's see how LLC and LCC react when the load is shorted or open.

When the load shorts, the voltage gain G_V dramatically drops. LLC may fall into the hard-switching region if the control loop cannot respond fast enough (the control bandwidth is normally around kHz level). But the LCC will not lose ZVS in this case because it maintains ZVS all the way down to gain = 0 independent of where the load current was before the load shorts. This can be seen in [Figure 6b](#).

When the load is disconnected, in other words, R_e soars; LLC's output voltage will not go wildly high, but LCC's will. Additionally, LCC may enter the hard-switching region as the voltage gain jumps. Therefore, LCC definitely requires an output OVP. ICL5102 has an OVP pin, which can be used to quickly protect against the output OVP by sensing the output voltage via an auxiliary winding that couples the secondary side. The output OVP is important for lighting ballast with SELV class (output is strictly less than 60 V).

2.2.3 Voltage gain range and frequency span

Let's check the voltage gain curves of LLC and LCC in [Figure 6](#); they are reproduced in [Figure 7](#). Here, for a fair comparison, the Z_e value is the same, the curves of the same color represent the same R_e value: $f_{RH,LLC} = f_{RH,LCC}$, and f_{HL} values are the same in both LLC and LCC figures. It can be found that although the maximum voltage gains are almost identical at the same load R_e , the minimum voltage gain of the LCC topology is smaller than that of LLC within the same frequency span (Δf). The reason is that once the frequency of LLC goes beyond its series resonant frequency $f_{RH,LLC}$, the voltage gain curve tends to become much flatter at the high load resistance. This exhibits the typical characteristics of a pure series resonant converter. Meanwhile, LCC operates in the vicinity of the parallel resonant frequency, where a more flexible voltage gain can be obtained.

Therefore, LCC covers a wide voltage range at the same frequency span and load range; in other words, LCC is a better choice in terms of the load operating range.

There are ways to enlarge LLC's voltage gain range. Without adding an extra resonant element or changing the duty cycle from 50 percent in the HB structure, compressing the ratio between $f_{RL,LLC}$ and $f_{RH,LLC}$ – in other words, reducing the ratio of L_p/L_s , is the solution commonly seen [\[3\]](#). However, the consequence will be that larger magnetizing current (reactive power) results in larger conduction loss in the transformer windings and MOSFETs. Therefore, there is a design trade-off in the LLC optimization between the efficiency and voltage gain range.

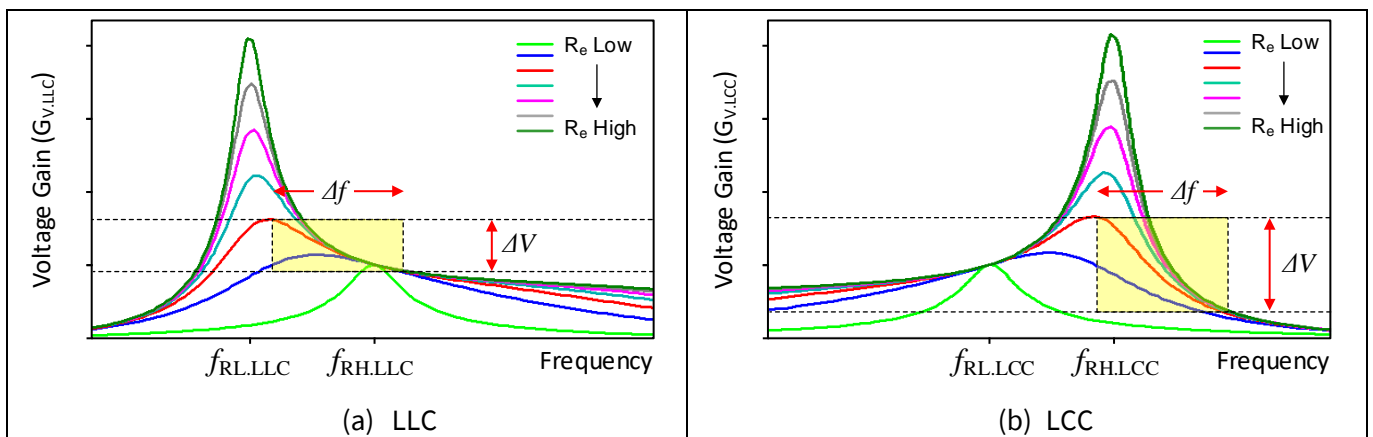


Figure 7 Voltage gain curves of (a) LLC and (b) LCC (curves of the same color show load resistance of the same value)

LLC vs. LCC

However, in applications where the input and output voltages are fixed, LLC can be designed at the series resonant point $f_{RH,LLC}$. At this point, LLC gives the best efficiency and moreover, its operating frequency under varying loads does not change, which facilitates the EMI filter design.

2.2.4 Voltage source vs. current source

Why do LLC and LCC behave so differently? Let's take a look at another state in the resonant tank. Using the J_{norm} equation in [Table 1](#), [Figure 8](#) plots the normalized load current of both topologies (top graphs) as well as the voltage gain (bottom graphs). It can be seen that, independent of load resistances, the LCC load currents converge at the higher resonant frequency $f_{RH,LCC}$, which represents the parallel resonance among three elements L_s , C_s and C_p . At this point, LCC looks like a stiff current source. On the other hand, LLC is like a voltage source at its $f_{RH,LLC}$.

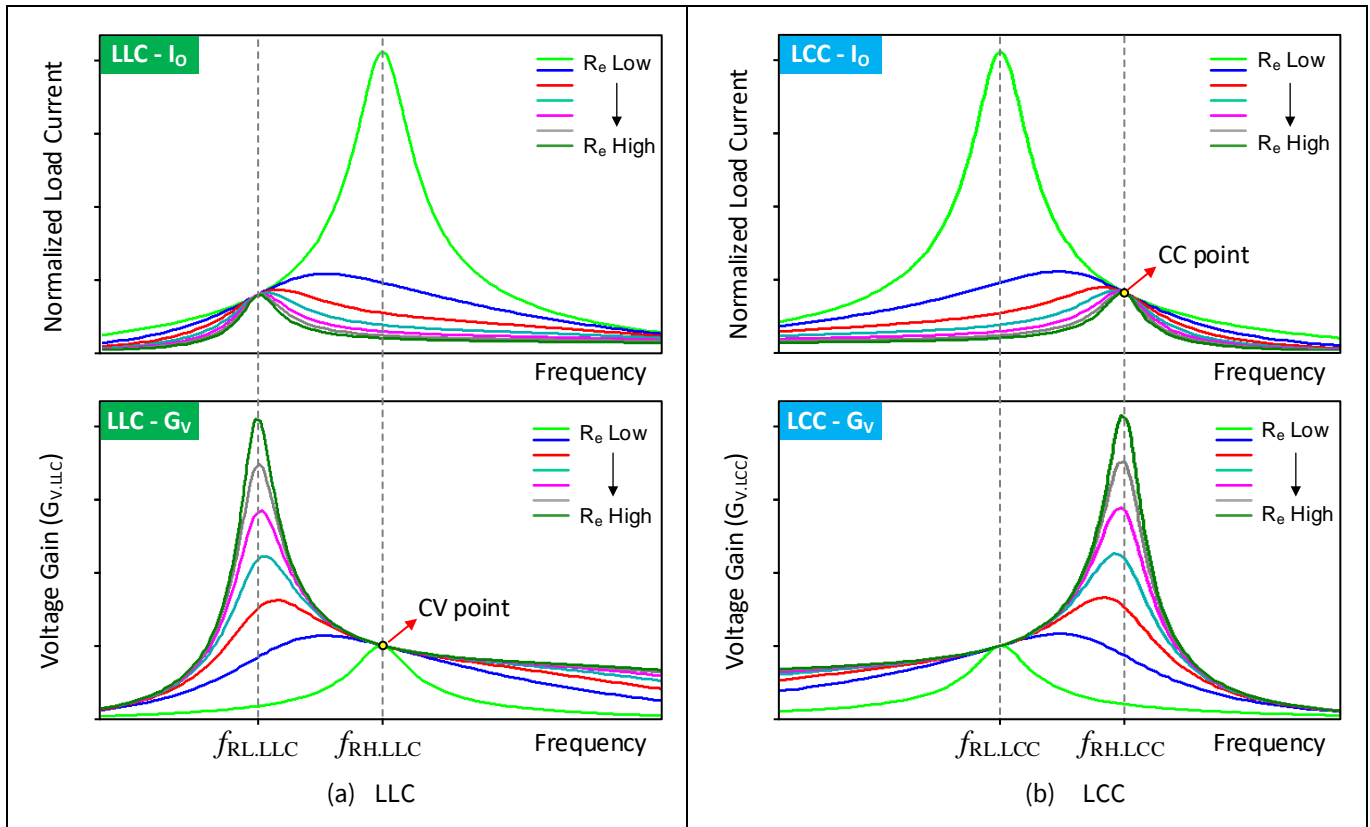


Figure 8 Normalized load current and voltage gain of (a) LLC and (b) LCC

This can be explained by the Thévenin and Norton circuit transformation, as shown in [Figure 9](#). It is well understood that at the series resonant frequency ($f_{RH,LLC}$) the impedance of C_s and L_s in series is zero, so the load R_e , no matter how big or small it is, sees a voltage source directly as indicated in the Thévenin equivalent circuit ([Figure 9a](#)). At this constant voltage (CV) point, one can design a low-cost PSR LLC with a CV output for applications where the input voltage is stable, and the accuracy and ripple of the output voltage are not highly demanding.

LLC vs. LCC

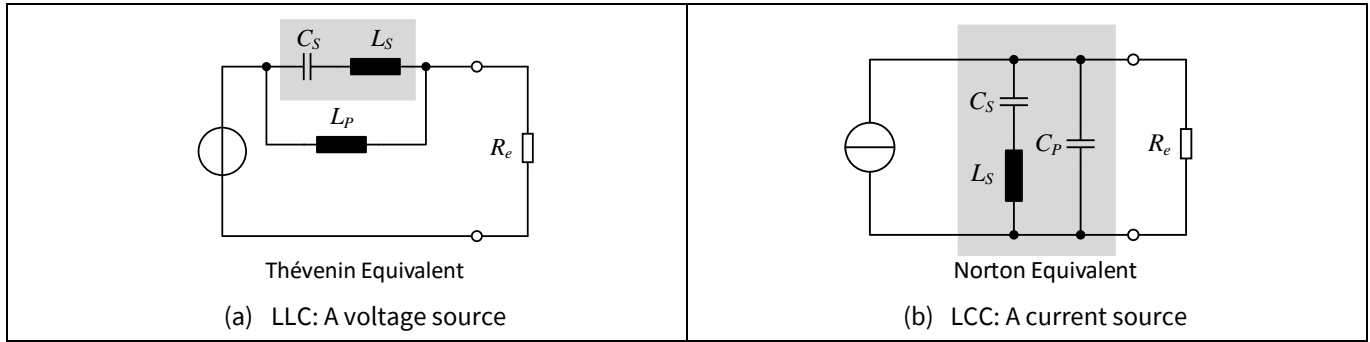


Figure 9 Equivalent circuit of (a) LLC and (b) LCC in the FHA

When operating near the parallel resonant frequency ($f_{RH,LCC}$), LCC can be more easily understood with the Norton equivalent circuit (**Figure 9b**). The impedance of the resonant tank at $f_{RH,LCC}$ is infinite. Therefore, the equivalent current source completely feeds the load, and its current value is nearly independent of the load. This is called the constant current (CC) point. That is the reason why LCC can support much wider output range. Utilizing this feature, a low-cost PSR LCC has been designed for a non-dimmable lighting application (see **section 5.3**). The key design challenge is about how to keep the output current spread within an acceptable level in such an open-loop control scheme.

Another important feature can be found in the normalized load current graphs in **Figure 8** – that at the same frequency span, LCC can handle much wider load current. Experience shows that LLC, when specified with a wide output voltage, must enter burst mode in the light-load condition. This is not welcome in lighting applications, because the induced low-frequency current ripple jeopardizes the light quality, and the potential audio noise can be difficult to solve. Large OEM lighting customers try to avoid entering burst mode for deep dimming. Therefore, LCC becomes an attractive candidate for applications with wide output voltage and current range.

2.2.5 Sensitivity to the parasitic capacitance

Parasitic elements in the resonant circuits can introduce extra resonance that distorts the circuit operation from the ideal state. The most prominent parasitics are the stray capacitances that reside within transformer windings and output semiconductors, like the output diodes or the MOSFETs in the synchronous rectification (SR) structure. These capacitances can be lumped as a capacitor in parallel with the magnetizing inductance L_P of the transformer.

Figure 10 illustrates the LLC voltage gain curves with and without the parasitic capacitance included. It can be seen in **Figure 10a** that the parasitic capacitance clearly raises the voltage gain as the load resistance goes very high (light-load operation) and the operating frequency rises. This not only results in a further frequency extension to obtain the same voltage gain, but also, more severely, drives the topology into hard-switching and control instability. Therefore, for an LLC converter with wide load range, it is recommended to set the frequency close to the series resonant point ($f_{RH,LLC}$) when the specified load current and voltage are minimal.

LLC vs. LCC

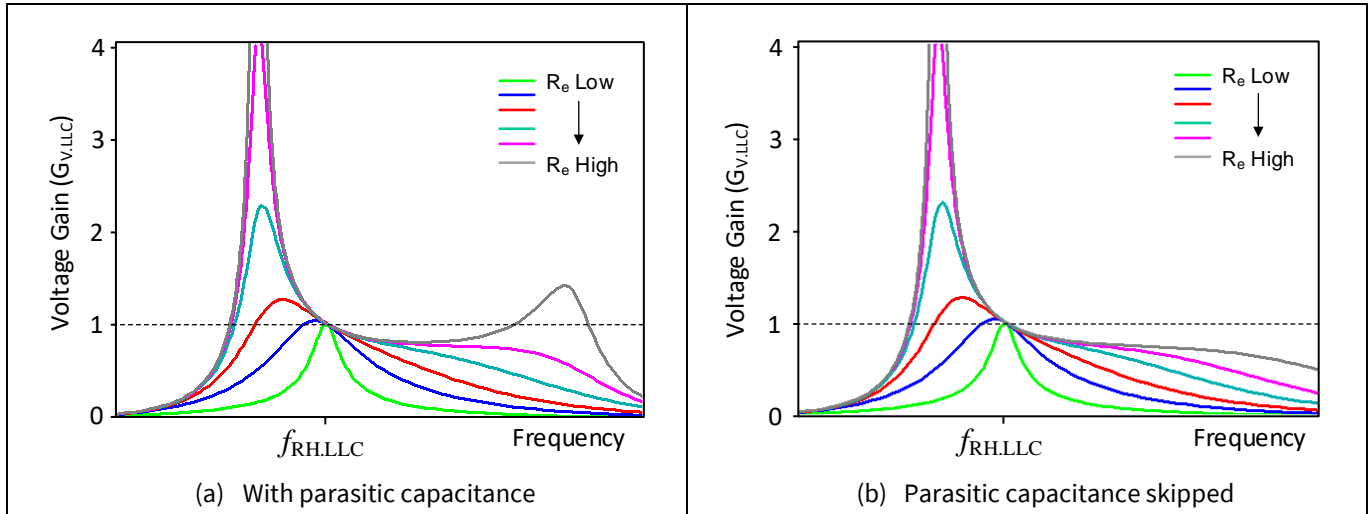


Figure 10 Voltage gain curves of LLC FHA models (a) with and (b) without the parasitic capacitance

On the other hand, this kind of parasitic capacitance does not obviously affect the LCC design and operation. If its parallel resonant capacitor C_p is placed across the transformer terminals on the secondary side, this parasitic capacitance is basically merged with C_p . Because of its much smaller value, the influence of the parasitic capacitance is insignificant.

2.2.6 Integrated transformer structure

With a discrete resonant inductor, the LCC tank design will have more freedom; however, utilizing the transformer leakage inductance as the series inductance helps to reduce the system size/BOM cost and simplify the inventory management.

The structures of the integrated transformers of LLC and LCC are different. **Figure 11** illustrates the symmetrical half of the structure of an integrated transformer. Here, the Litz wires are used for both primary and secondary windings. To achieve sufficient leakage inductance, the primary and secondary windings are normally placed into different sections of the bobbin.

Once the wire types and winding turn numbers have been fixed according to the design principle, current rating and so on, the distance between two winding sections (L_{bg} in **Figure 11**) needs to be adapted for proper leakage inductance. This is the same for both LLC and LCC.

The magnetizing inductance of the LLC transformer must be finite compared to its leakage, so the air gap in the center core leg (L_{ag} in **Figure 11**) must be created to manipulate the value of L_p . Meanwhile, this air gap is not absolutely necessary for the LCC transformer because its magnetizing inductance can be much larger than its leakage. This means the LCC transformer is easier and cheaper to make. Moreover, the winding loss induced by the fringing field around the air gap may be an issue in the LLC integrated transformer, but not in the LCC.

LLC vs. LCC

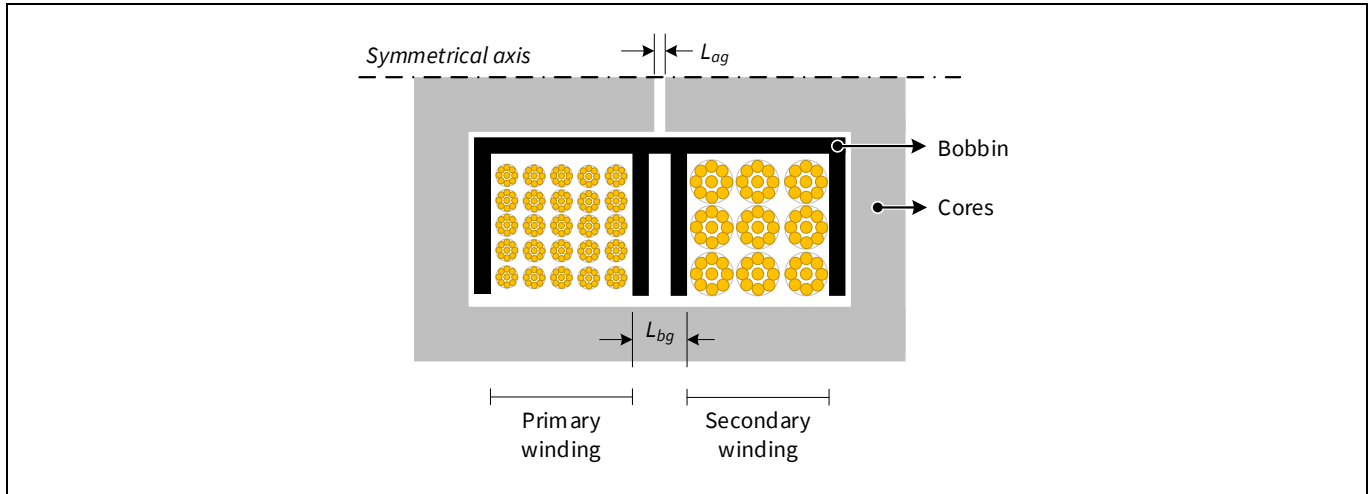


Figure 11 Structure of an integrated transformer concept for LLC and LCC converter

It should be noted that once an integrated transformer is used, the designers can only place the parallel resonant capacitor C_p on the transformer secondary side. For applications with LV output, this generally reduces the capacitor cost due to the smaller voltage rating.

2.2.7 Light-load loss

As the operating frequency goes high in the light-load case (if the system does not enter burst mode), both converters have higher core loss. Meanwhile, LCC still needs to charge C_p to the same output voltage. This means the circulating energy becomes higher at light load, and it will further deteriorate the system efficiency. Therefore, using continuously operating LCC for applications that demand high system efficiency at light load is not recommended.

2.3 Summary

This chapter compares the characteristics of LLC and LCC topologies using the FHA approach. It shows that LCC outperforms LLC in the following ways:

- Wide voltage range thanks to its current-source-like behavior
- Much wider load current range in the same frequency span, which means an LED driver with wide output voltage can dim very deeply without using troublesome burst mode
- Robustness against output short-circuit
- Less immunity to parasitic capacitance
- Easier integrated transformer design

However, LCC also has several drawbacks:

- Output OVP is compulsory
- Higher light-load loss than LLC
- One extra parallel resonant capacitor is used

3 LCC operation and design guidelines

This chapter first takes a close look into two main LCC operating modes and presents design guidelines for an efficient LCC converter.

3.1 Operation modes

Like LLC, LCC is also a load-resonant topology driven by a square voltage wave with 50 percent duty ratio. It has two main operating modes in the soft-switching range, which is simpler than LLC [4]. Figure 12 shows the schematic of an LCC converter with the parallel resonant capacitor C_P placed on the primary side of the transformer. In the following parts the operation of these two LCC modes is described.

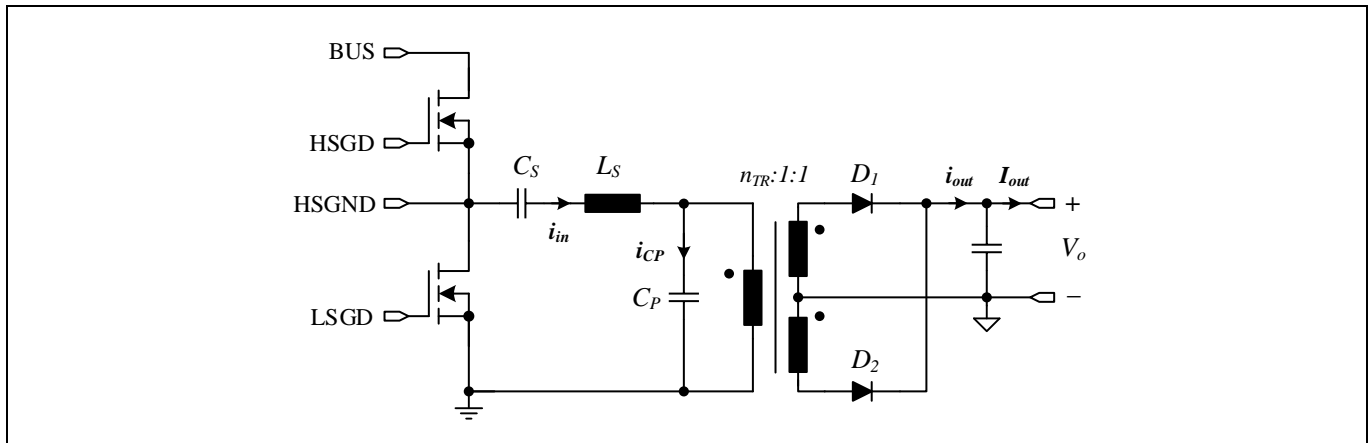


Figure 12 HB-driven LCC circuit

3.1.1 High-power mode

In a soft-switching operation, the resonant tank current (i_{in} in Figure 12) has to lag behind the input voltage V_{HSGND} . In the high-power mode, the phase lag is relatively smaller than the lower-power mode, which will be shown later. Figure 13 describes the key waveforms and the equivalent circuit of each time interval.

- **t_0 to t_1 (T_A):**

The high-side (HS) switch is turned on, so the tank current i_{in} goes up from 0 A and the voltage across C_P swings from negative polarity to positive. Here, all three resonant elements, C_S , C_P and L_S , resonate. Due to the need to turn around the voltage polarity of the V_{CP} , all the resonant tank current must flow into C_P instead of flowing to the load. Therefore, the output diodes do not conduct during this time interval and no energy is delivered to the output. T_A is also known as the output diode blanking time.

- **t_1 to t_2 (T_B):**

The output diode conducts once the voltage across C_P (V_{CP}) reaches the output voltage (referred value to the primary side). Here, only the two resonant elements C_S and L_S resonate.

- **t_2 to t_3 (t_{DT}):**

This is the dead time of the HB. The HS switch is turned off, but the low-side (LS) switch is not on yet. To realize the ZVS operation, the inductor current I_{off} at t_2 should be high enough to drain out the energy stored in the lumped capacitance C_{eq} at the HSGND node within the maximum dead time.

- **t_3 to t_4 (T_C):**

The LS switching is on, but the voltage across C_P is still high. Here, only the two resonant elements C_S and L_S resonate.

In the high-power mode, the current of the output diodes looks like a quadrangle. Due to the existence of the blanking time (T_A), the current shape of the output diodes should be designed with less RMS value to deliver the same average current for an efficient operation.

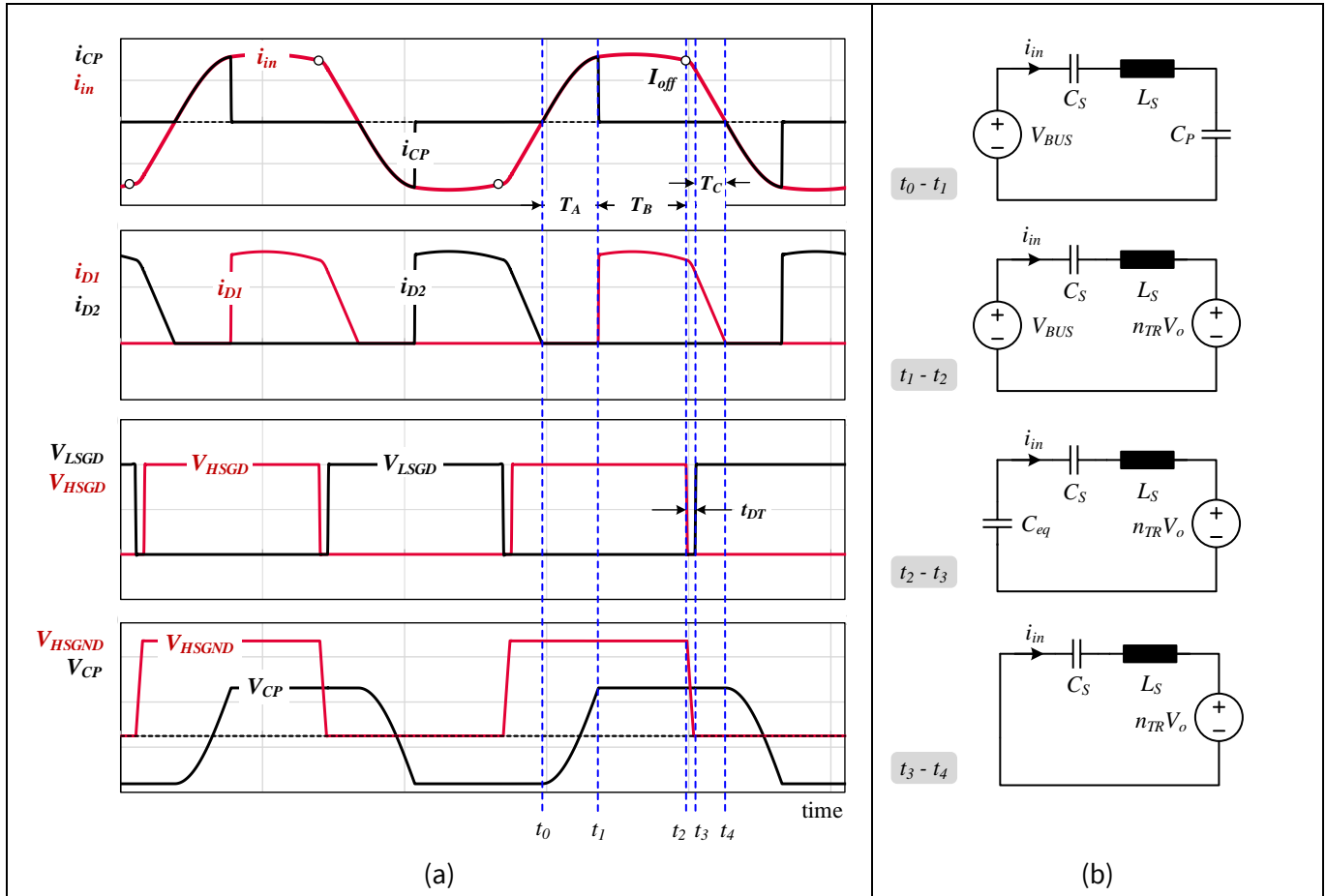


Figure 13 High-power mode: (a) key waveforms and (b) equivalent circuit in each time interval

3.1.2 Low-power mode

As the operating frequency rises and the load drops, the phase shift between the tank input voltage and current extends, and the time interval T_B (t_1 to t_2 in Figure 13a) gradually reduces. As $T_B = 0$, LCC will enter low-power mode.

- **t_0 to t_1 (T_A):**

During the on-time of the HS switch, the tank current i_{in} rises from zero until the HS switch is turned off on t_1 . The V_{CP} starts rising from the negative output voltage (referred value to the primary side). At t_1 , V_{CP} has not yet reached the positive rail.

- **t_1 to t_2 (t_{DT}):**

This is the dead time of the HB. The HS switch is turned off, but the LS switch is not on yet. Here, four elements are resonating (C_S , C_P , C_{eq} and L_S).

- **t_2 to t_3 (T_B):**

The LS switch is turned on and the tank still resonates (C_S , C_P , and L_S).

- **t_3 to t_4 (T_C):**

Once the V_{CP} reaches the output voltage at t_3 , the output diode conducts and the output voltage further reduces the tank current to zero, until t_4 .

In this operating mode, the output diode current has a triangular shape. This is apparently not an efficient way to transfer the energy at full load.

The waveforms of the high-power mode can be described by analytical equations, but those of the low-power mode can be only calculated numerically [5].

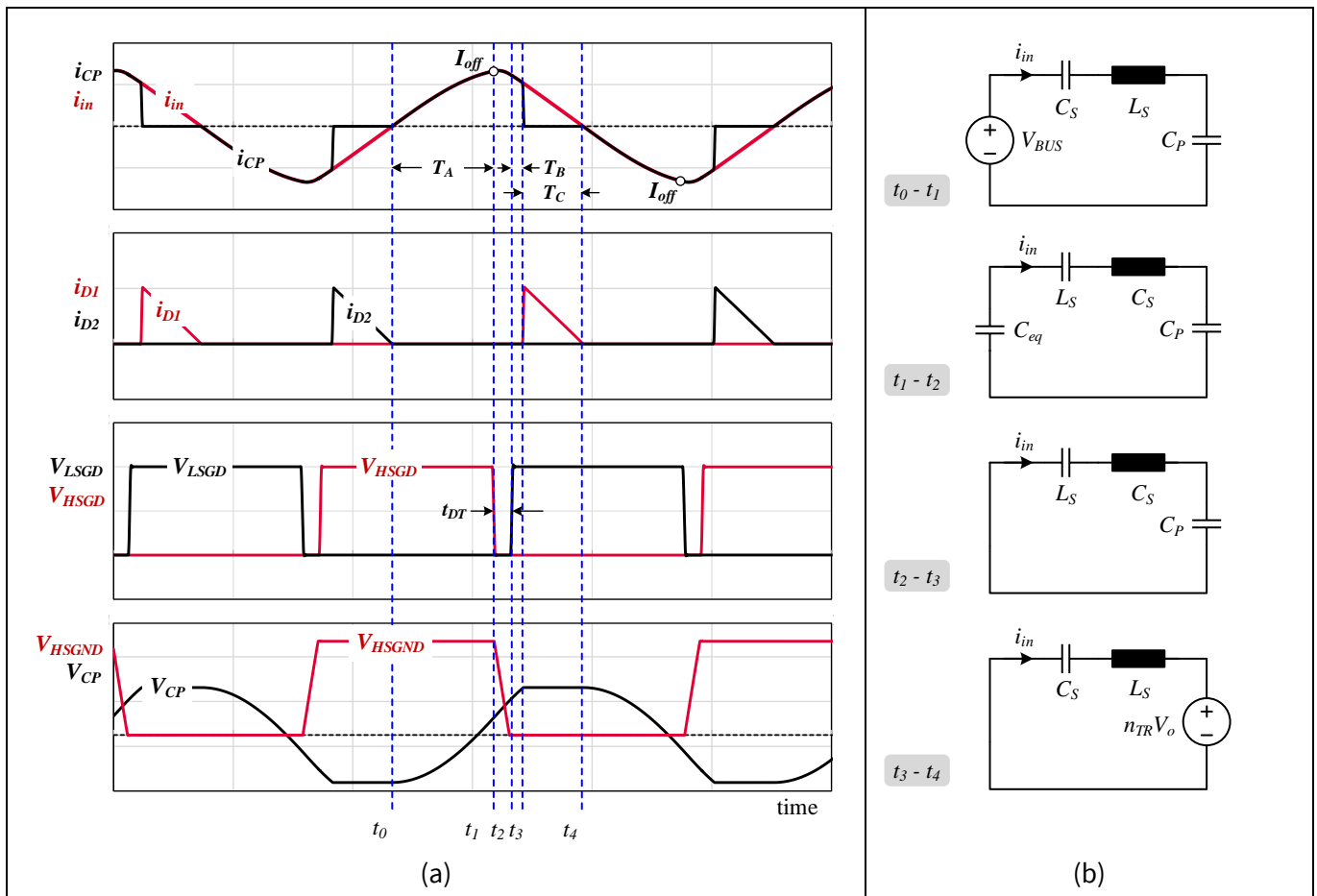


Figure 14 Low-power mode: (a) key waveforms and (b) equivalent circuit in each time interval

3.1.3 Zero-power mode

In many applications the load could be close to zero power. As the frequency keeps increasing, the voltage across the parallel resonant capacitor becomes lower than the output voltage at a point, and then the output diodes will not conduct any more, which indicates zero output power. At this point, the LCC circuit becomes linear again. With given resonant tank parameters, and input and output voltages, one can analytically calculate the frequency at which the output power is zero. **Figure 15** illustrates the key waveforms in this zero-power state, where it can be found that the current into the C_P becomes sinusoidal. Being able to analytically calculate the parameters of this state is important for the LCC resonant tank design. This will be addressed in **section 4.1**.

LCC operation and design guidelines

It is worth mentioning again that when the output is shorted (also a kind of zero-power state) or the output voltage dramatically drops, LCC will still operate in a soft-switching region as shown in **Figure 6b**. This is different from LLC if the controller cannot react quickly enough.

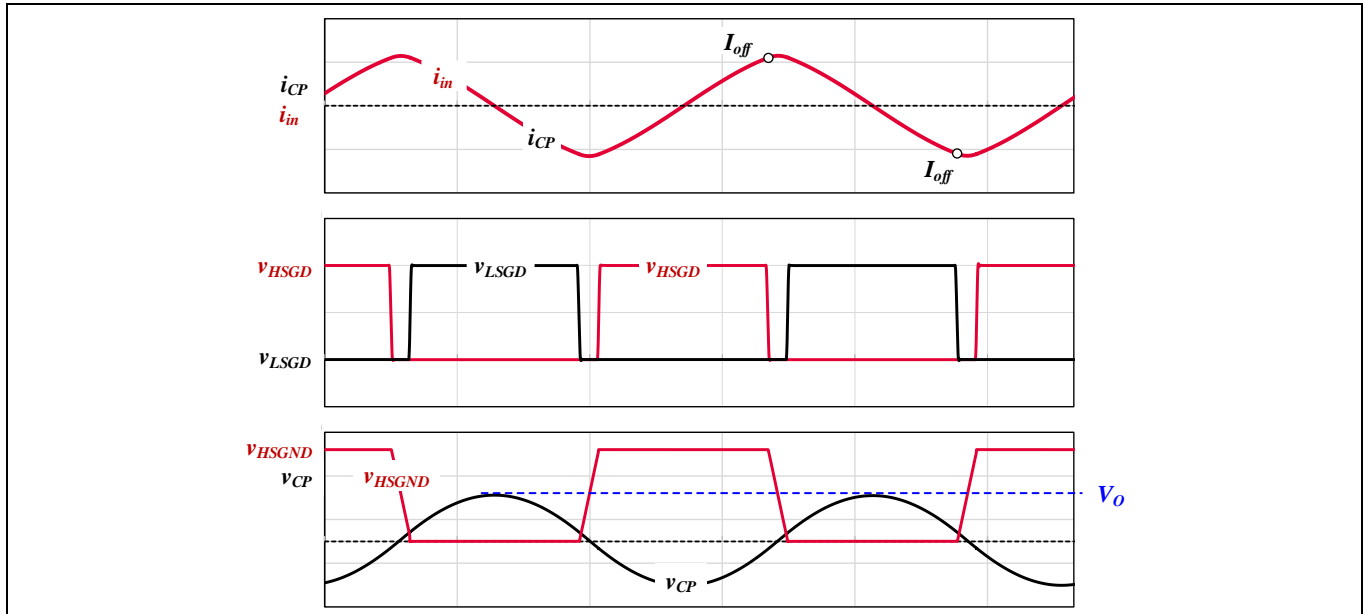


Figure 15 Zero-power mode – key waveforms

3.2 A practical design rule for an efficient LCC converter

This part will introduce a practical design rule for an efficient LCC converter.

3.2.1 Efficiency indicator of an LCC converter

Due to the existence of the parallel resonant capacitor C_p , the output diodes (D1, D2 in **Figure 12**) of the LCC converter always have a blanking time (time interval T_A in **Figure 16**) during which the transformer current i_{in} only charges C_p without flowing into the output. This is similar to DCM in the LLC when its operating frequency is smaller than its resonance frequency. The energy circulating within the resonant tank during T_A not only causes extra conduction loss, but also reduces the effective time (T_B , T_C) of delivering energy to the load. In a fixed switching period, smaller $T_B + T_C$ means higher RMS current value of output diodes (i_{out} in **Figure 12**) at the same load current (I_{out}); in other words, larger conduction loss in the output diodes and transformer windings.

To quantify how effectively the energy is delivered to the output, a meaningful efficiency indicator of the LCC converter can be defined as the ratio between the RMS value of i_{out} and the DC load current I_{out} :

$$RMS/AVG = \frac{RMS(i_{out})}{I_{out}} \quad \text{Eq. 4}$$

In general, the smaller this ratio is, the more efficient the conversion will be.

LCC efficiency is pretty good when this value is between 1.2 and 1.3. For reference: when the LLC operates at its resonant point where its efficiency is normally considered to be the highest, its i_{out} looks like a rectified sinusoidal current only with a little blanking time (originated from the dead time of the HB switching). In this case, its **RMS/AVG** value is about 1.11 ($0.5\pi/\sqrt{2}$). However, it is worth mentioning that an LLC converter, specified with wide output voltage and current operating range, cannot operate at its resonant point at full load, so 1.11 is only an ideal value for such a resonant converter.

3.2.2 A practical design rule for high efficiency at full load

To minimize **RMS/AVG** ratio, designers must realize an efficient i_{out} current shape. An optimal i_{out} shape could be trapezoidal, as shown in **Figure 16**. A trapezoidal shape with small blanking time T_A is close to an ideal DC current. Another reason to choose the trapezoidal shape is that it is practical and straightforward to design. Let's see how to achieve a trapezoidal i_{out} shape at full load.

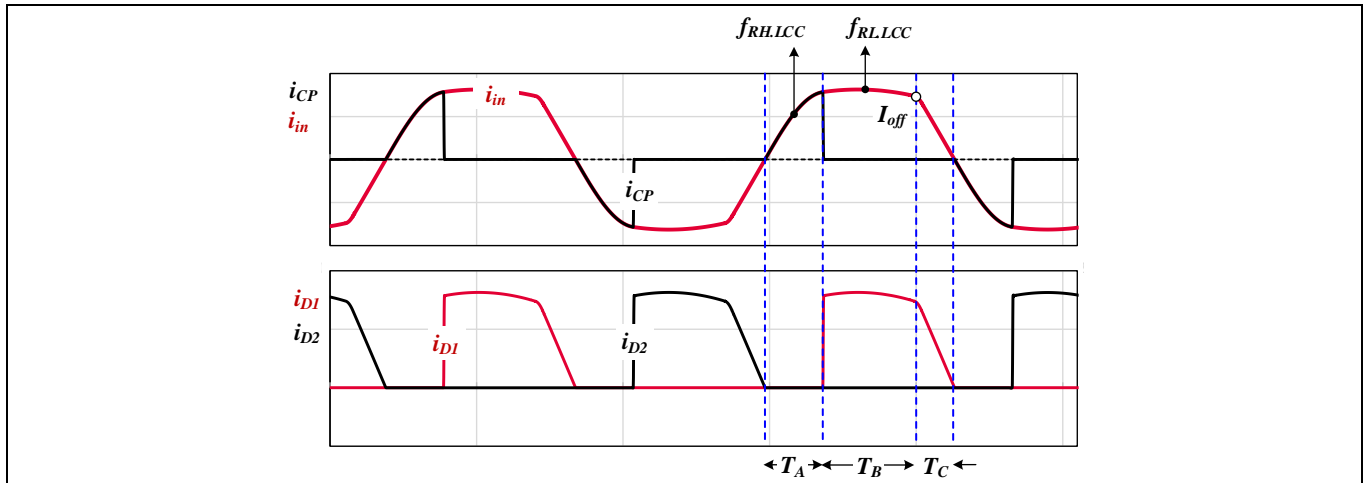


Figure 16 Key waveforms of an efficient LCC in high-power mode

- T_A internal (t_0 to t_1 in **Figure 13**):

C_p is charged and three elements resonate with the frequency of $f_{RH.LCC}$ in the internal. To make T_A a small ratio within the switching cycle, $f_{RH.LCC}$ should be much larger than the switching frequency f_s . Normally, the switching frequency to realize light load (e.g., 1 percent dimming in lighting) is higher than $f_{RH.LCC}$, which implies that an efficient LCC with wide load requires a wide frequency range.

$$f_{RH.LCC} \gg f_s \quad \text{Eq. 5}$$

- T_B internal (t_1 to t_2):

Here, two series resonant elements (L_s , C_s) resonate. To make the current shape flat, two conditions should be fulfilled:

1. The switching frequency f_s should be larger than $f_{RL.LCC}$.

$$f_s > f_{RL.LCC} \quad \text{Eq. 6}$$

The larger the ratio $f_s/f_{RL.LCC}$, the flatter the current shape will be.

2. The transformer turns ratio N_{TR} should be equal to the ratio between the half-bus voltage V_I ($V_{BUS}/2$) and the maximum output voltage V_{Omax} .

$$N_{TR} = \frac{V_I}{V_{Omax}} \quad \text{Eq. 7}$$

- T_C internal (t_3 to t_4):

Here, two series resonant elements (L_s , C_s) still resonate, but the input voltage to the resonant tank becomes zero.

In some applications where a constant maximum output power applies in a range of output voltages, N_{TR} selection according to [Eq. 7](#) will result in an i_{out} shape bending upward in internal T_B when the output voltage is lower than $V_{o,max}$ (see [Figure 17a](#)). Experiments and calculations have shown that in this case, the **RMS/AVG** ratio further improves at the same power because of a smaller T_A . Additionally, the current I_{off} ([Figure 17](#)) at which the switch is turned off becomes larger, meaning the ZVS realization is not a problem. Once the N_{TR} is selected to be larger than [Eq. 7](#), the current will bend downward ([Figure 17c](#)). In this case, the current goes forward to a triangular shape, which causes higher RMS/AVG ratio and hence, higher loss. An N_{TR} value slightly larger than [Eq. 7](#) can be used to enable some design freedom. However, care should be taken because a very large N_{TR} , I_{off} may be too small to realize ZVS.

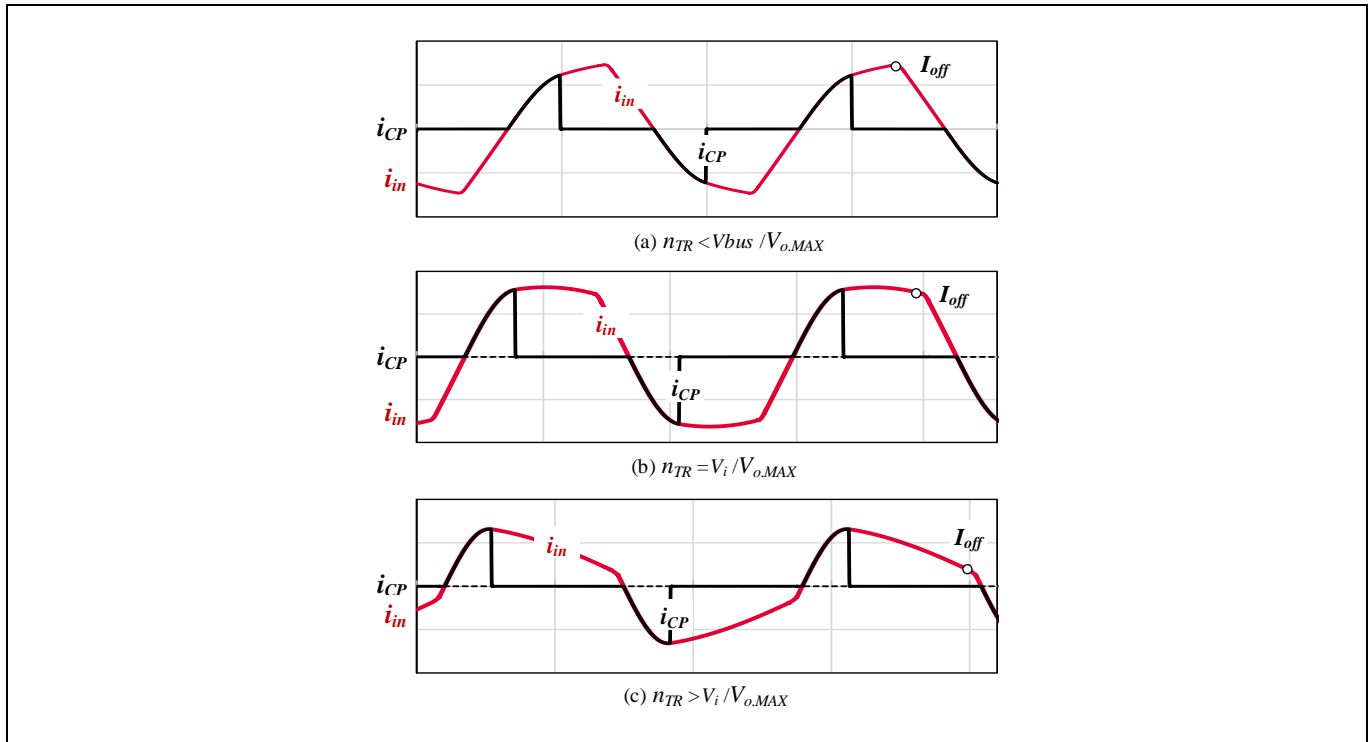


Figure 17 Resonant tank current at different transformer turns ratios

According to [Eq. 5](#), [Eq. 6](#) and f_{HL} equation in [Table 1](#), it can be concluded that an efficient LCC requires the C_S/C_P ratio to be large. This makes sense, because smaller C_P results in less circulating energy. Once $f_{RH,LCC}$ is far apart from $f_{RL,LCC}$, it also implies that the LCC operating frequency range must be wide to cover a wide load range, because the frequency to achieve zero power at the lowest output voltage is higher than $f_{RH,LCC}$.

This practical design rule is not sufficient to fix all related parameters, so the next chapter will introduce an accurate and easy-to-use LCC design tool to quickly set the resonant tank parameters.

4 Design tool for LCC with wide load range

The prerequisites of an accurate FHA-based design approach are:

- a sinusoidal input current into the resonant tank that is in phase with the input square voltage, and
- continuous conduction of the output diodes.

However, LCC operation obeys neither of these. Therefore, the FHA approach is not easy to use for a precise LCC design. Several iterations are necessary to reach a satisfactory result. Additionally, this approach provides no information about how relatively efficient the design is.

We have developed an accurate, time-saving and easy-to-use LCC design tool which is based on time-domain analysis (TDA) equations built in MathCAD™ version 15. Infineon customers can use it to swiftly calculate four parameters of the LCC resonant tank, C_P , C_S , L_S and N_{TR} , for efficient operation in high-power mode. Users must keep in mind the specified input and output voltage ranges, power level and desired frequency range.

Note: Currently, please ask our local FAE colleagues to support LCC calculation with this design tool.

4.1 Working principle

The goal of this LCC design tool is to analytically calculate four parameters of the LCC resonant tank (C_P , C_S , L_S and N_{TR}) for a low **RMS/AVG** ratio within the given specification of input/output voltage range, power range and desired frequency range.

We have four unknown parameters here. First, the turns ratio N_{TR} can be set by Eq. 7. Then, we still have to construct three independent equations to calculate C_P , C_S and L_S . These three relations are:

- **Zero power** at the minimum output voltage and virtual maximum frequency.

Both LLC and LCC generally have a wide frequency span as the specified output voltage range is wide. The specified maximum frequency will constrain one of the C_P , C_S and L_S relations. Frequently, in LED indoor lighting applications, the minimum load can be 1 percent of the maximum value. Meanwhile, this value can be 10 percent or less in the battery charger and outdoor lighting applications. LCC in light load such as 1 percent to 10 percent already works in low-power mode, which can only be described numerically. In these cases, not far away from this deep light load, zero-power mode of LCC can be analytically calculated. Designers could just assume a virtual maximum frequency that achieves zero power. It is only called “virtual” because most likely no specification requires zero power. This virtual frequency can be selected to be just slightly bigger than its desired real maximum frequency that realizes the specified minimum power.

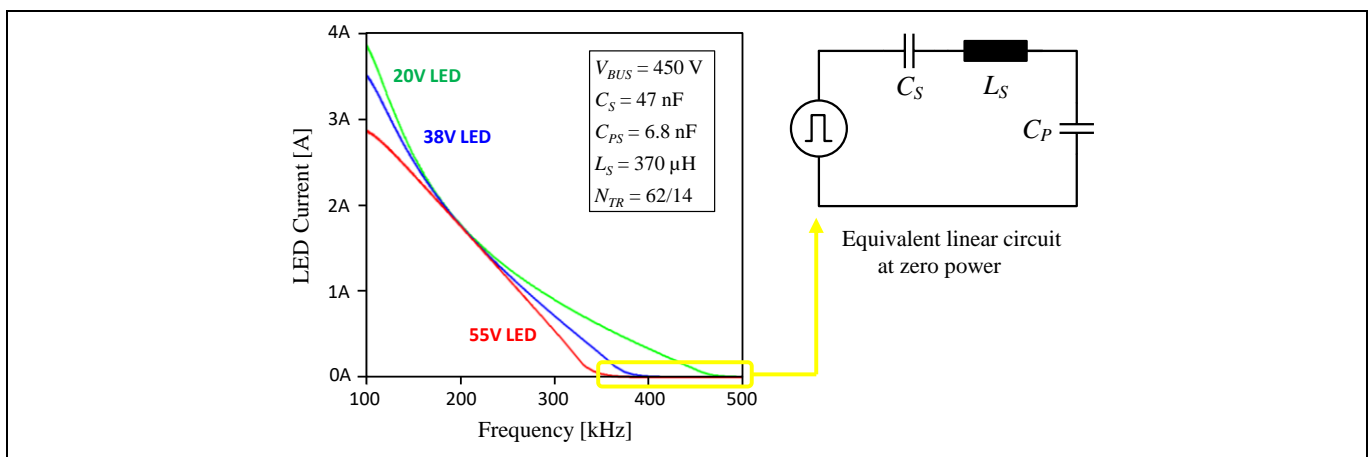


Figure 18 LED current scan of a 100 W design and the linear equivalent circuit at zero-output power

Design tool for LCC with wide load range

This virtual maximum frequency for zero power occurs at the minimum output voltage. **Figure 18** shows the LED current scan as a function of the LCC switching frequency and LED voltage in a 100 W design (LCC parameters are given in the legend). At the zero-power region, the equivalent circuit is as simple as an input voltage source connected with capacitors and the inductance. It can be seen that the maximum frequency achieving zero power happens on the low LED voltage, while the minimum frequency for the maximum power is at the high LED voltage.

- **Maximum power** at the specified maximum output voltage and minimum frequency.

Selection of the minimum frequency depends on many design considerations, such as the desired transformer size, or efficiency or ease of solving EMI. As shown in **Figure 18**, the minimum frequency for maximum power occurs at the maximum output voltage. The lowest end of the frequency span also constrains the C_p , C_s and L_s relation. As mentioned before, the high-power mode can also be calculated analytically. In this LCC design tool, the waveforms of each phase in the high-power mode are described with second-order differential equations, and the initial conditions of each phase are found with the state-plane-analysis approach.

- **RMS/AVG value** at the maximum load.

The last constraining relation is chosen to be efficiency related. The **RMS/AVG** value gives designers a reference for how efficient their selected parameter set is, relative to other choices. The RMS current value of i_{out} is calculated based on the analytical waveform equations.

With these three equations, we construct two design charts from where the LCC resonant tank parameters can be selected. How to use these design charts will be described in **section 4.3**. First, the assumption, input and output of this tool will be introduced below.

4.2 Assumption, input and output of this tool

4.2.1 Assumption

Several assumptions have been made to simplify the calculation but still guarantee sufficient accuracy. These assumptions are as follows:

- A PFC stage controlling the bus average voltage constant is present in front of the LCC stage.
- No magnetizing current in the transformer; namely, the impedance of the magnetizing inductance is much bigger than the load.
- Zero dead time of the HB.
- Zero loss in the power components, like MOSFETs on the primary side and the transformer. However, the voltage drop across the output diode or SR MOSFETs can be included in the tool for higher calculation accuracy in case of LV and high-current application.
- Input and output voltages are pure DC.

4.2.2 Input and output

The figure below is a flow chart for using this design tool. First, customers need to input the specified values:

- V_{BUS} : The average bus voltage controlled by the PFC stage.
- V_{Omin} : The minimum output voltage.
- $V_{Omax.Pmax}$: The maximum output voltage at the maximum load.

Design tool for LCC with wide load range

- $f_{Pmax.Omax}$: The minimum LCC frequency at the maximum power and maximum output voltage.
- $f_{max.0W}$: The maximum LCC frequency that results in zero power at the minimum output voltage.
- P_{Omax} : The maximum output power.
- L_{lk} : In case an integrated LCC transformer is required, designers should have an idea about how much leakage inductance the desired transformer shape can realize from a given power and voltage level. This value is not an input parameter for equation calculation, but more like a range from which the L_s should be selected.

After these parameters have been specified in the design input region, the tool starts the calculation. The process to obtain the optimized parameters will be described in [section 4.3](#).

This tool generates two types of output:

- Four LCC resonant tank parameters that are optimized for good efficiency (C_P , C_S , L_S and N_{TR}).
- Transformer input current waveform at full load for verification. This waveform can be used to check if the current waveform is the desired trapezoidal shape.

The design flow chart of this LCC design tool is shown in [Figure 19](#).

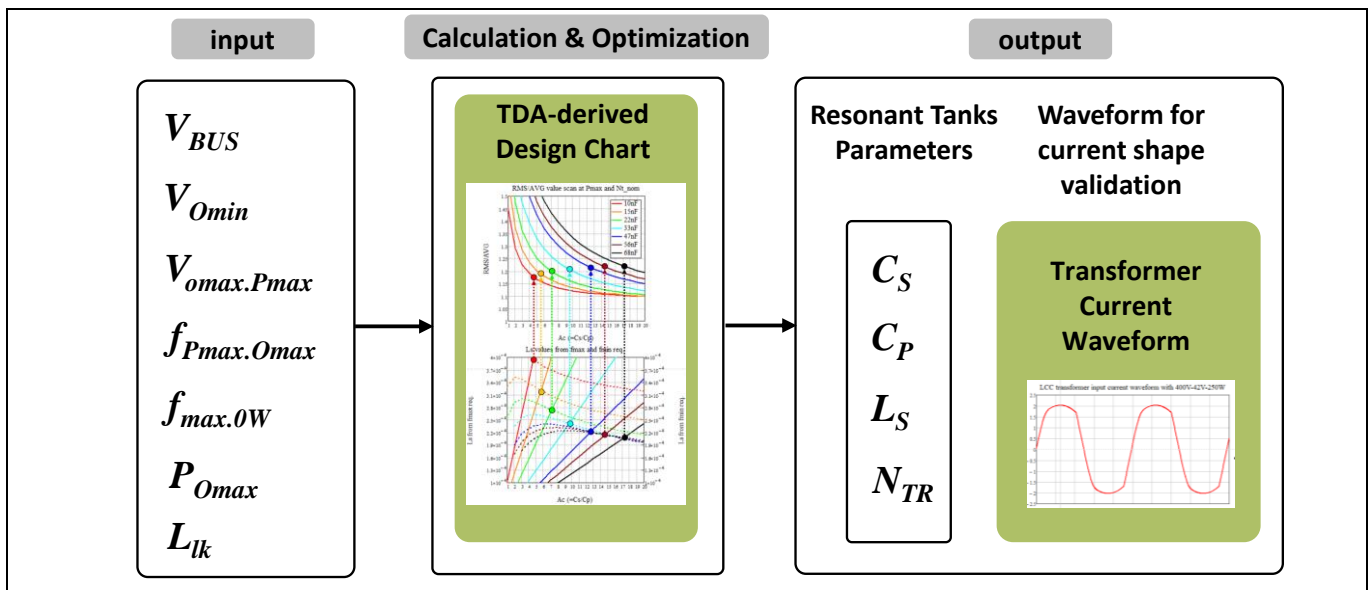


Figure 19 Design flow chart of the LCC design tool

4.3 Design charts

The most critical step in this tool is to derive the optimized LCC parameters from two TDA-derived design charts. One chart of the **RMS/AVG** shows values as functions of C_S and C_P , and the other shows the L_S values derived from the requirement for the maximum power with minimum frequency and from the requirement for zero power with the maximum frequency.

4.3.1 RMS/AVG chart

The **RMS/AVG** value is calculated as follows:

$$RMSAVG(V_{Omax.Pmax}, V_i, V_{Omin}, P_{Omax}, f_{Pmax.Omax}, f_{max.0W}, C_S, A_C, N_{TR}) \quad \text{Eq. 8}$$

Here the first six parameters are the specified inputs, and the last three are the design variables to calculate. A_c is the ratio between the C_s and C_p (see Eq. 9). N_{TR} is given as Eq. 7.

$$A_c = \frac{C_s}{C_p} \quad \text{Eq. 9}$$

In the **RMS/AVG** chart, Eq. 8 is plotted at several standard C_s values in a range of A_c . Figure 20 provides an example of the **RMS/AVG** chart. Seven **RMS/AVG** equations are placed in the arguments, giving seven different **RMS/AVG** curves with each representing one standard C_s value. Here, the X-axis is the A_c values. In the chart arguments, users are free to change C_s to the value of their interest.

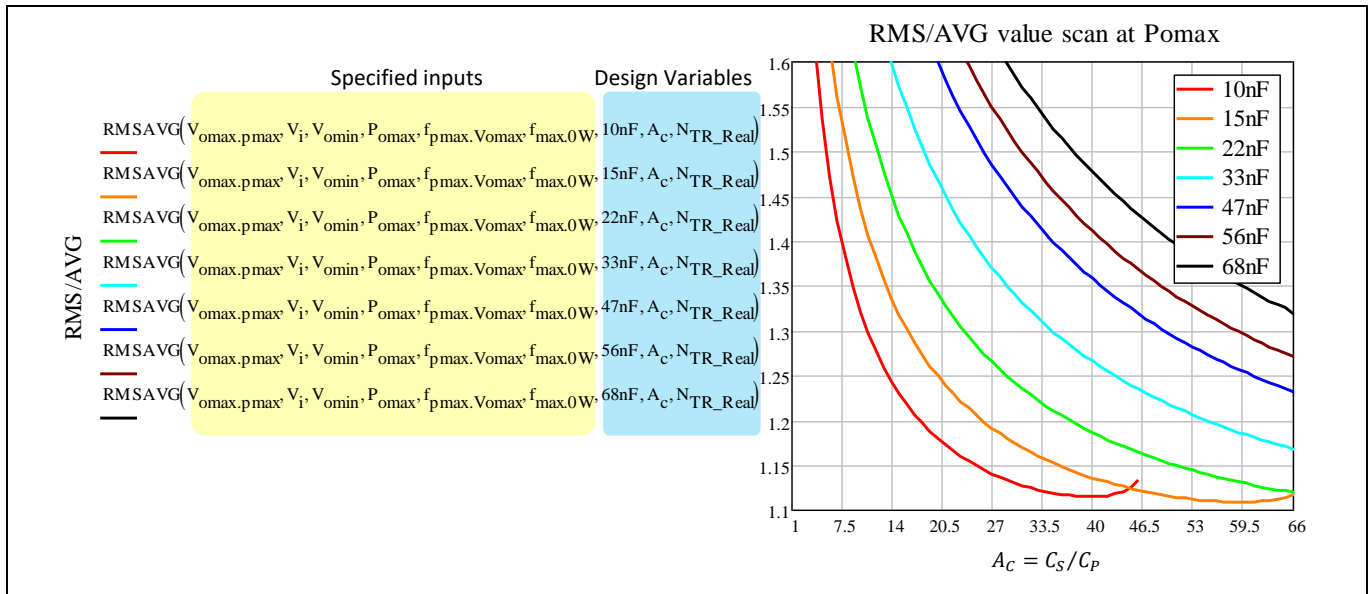


Figure 20 Example of RMS/AVG chart (legend shows different C_s choices)

It can be observed in Figure 20 that:

1. Larger A_c results in a smaller **RMS/AVG** value. This is in line with the statement in section 3.2.2: “an efficient LCC requires the C_s/C_p ratio to be large”. This chart provides a relative indication of the system efficiency among different choices of C_s and A_c .
2. No L_s information is required to obtain the **RMS/AVG** value. C_s and C_p can already decide the relative shape of the output diode current (i_{out}), which is enough for RMS/AVG calculation. However, we do need the L_s value to converge to the specified power at the desired frequency. This is why we must construct the L_s chart.

4.3.2 L_s chart

The L_s chart consists of two types of curves. One curve represents the L_s that achieves the maximum power P_{omax} at the specified maximum output voltage $V_{\text{omax.pmax}}$ and minimum frequency $f_{\text{pmax.0max}}$, and the other curve is for zero power at the minimum output voltage V_{omin} and virtual maximum frequency $f_{\text{max.0W}}$.

The L_s equation for zero power is in the form shown in Eq. 10:

$$L_{s_{0W}}(V_{\text{omin}}, V_i, f_{\text{max.0W}}, C_s, A_c, N_{\text{TR}}) \quad \text{Eq. 10}$$

The L_s equation for the maximum power is in the form illustrated in Eq. 11:

$$L_{S_Pmax}(V_{Omax.Pmax}, V_i, V_{Omin}, P_{Omax}, f_{Pmax.Omax}, f_{max.0W}, C_S, A_C, N_{TR})$$

Eq. 11

These two L_S functions are plotted on the left and right axis with the same display range; again, with the same discrete C_S values and A_C display range as the **RMS/AVG** chart.

Figure 21 illustrates an example of this L_S chart. The solid curves are the L_{S_0W} and the dashed curves are L_{S_Pmax} . Here, the same color in both L_S and **RMS/AVG** charts shares the same C_S value. The crossing points of the two curves of the same color represent the L_S , C_S and A_C values that are able to fulfill both the maximum-power and zero-power requirements. Here, the display scales of both Y-axes should be identical.

It can be noted the L_{S_Pmax} curves may stop at certain points, because the LCC will operate in low-power mode in the region beyond. The tool is made to automatically detect the boundary between high-power mode and low-power mode.

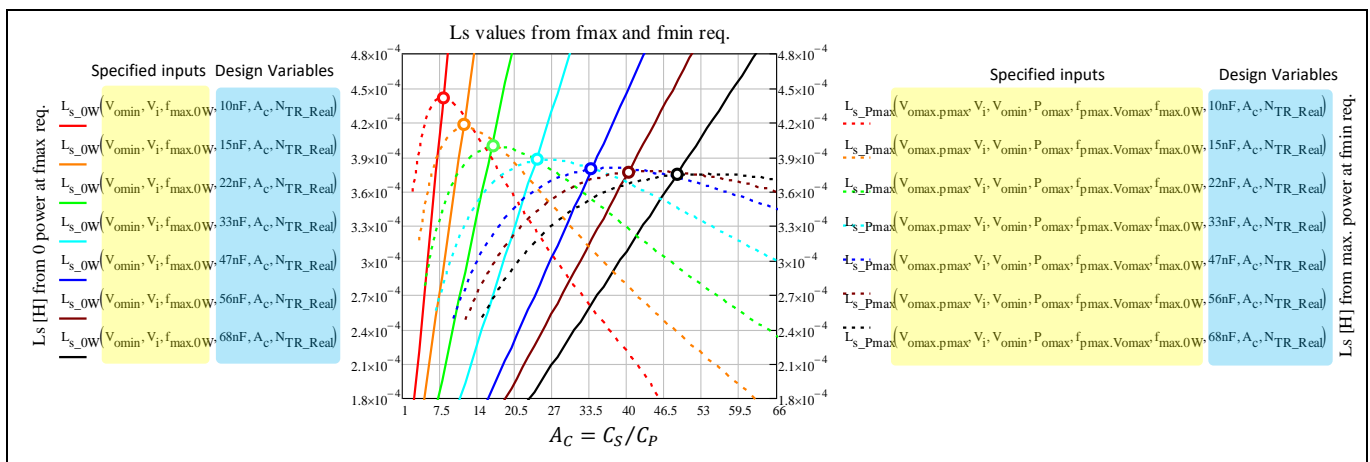


Figure 21 Example of L_S chart

4.3.3 Extraction of optimal parameters

It can be seen from the L_S chart that different C_S has its own C_P and L_S values to fulfill the given specification. They form different parameter sets. The question is which parameter set to choose.

If we combine the **RMS/AVG** chart with the L_S chart, we can get a hint about which parameter set is more efficient. **Figure 22** maps two charts together. These two charts are calculated based on the following specifications (**Table 2**):

Table 2 Key specifications of a 100 W LCC design (details seen in [section 5.2](#))

LCC parameters	Specification
Bus voltage	450 V
Max. output power (at max. output voltage)	100 W
Min. putput power (at min. output voltage)	1 W
Max. output voltage	55 V
Min. output voltage	20 V
Desired frequency at max. power	180 kHz
Desired frequency at zero power	450 kHz
Transformer core set	EFD25.4/19/9
	Integrated LCC transformer

Design tool for LCC with wide load range

The design choices at different C_s values in the L_s chart are projected into the **RMS/AVG** chart. From the example given in [Figure 22](#), it can be seen that a smaller C_s value gives a lower **RMS/AVG** value, but not by much. However, the L_s value at smaller C_s bends upward quickly. In this 100 W design, an integrated LCC transformer is required. The desired transformer shape is an EFD25.4/16/9 (see its dimensions in datasheet [\[6\]](#)). In a preliminary check, the maximum leakage inductance L_{lk} this transformer can achieve is around 400 μH , with the Litz wire that can handle the proper turns ratio and sufficient current rating. Therefore, parameter sets with C_s greater than or equal to 33 nF are in scope. Considering the transformer manufacture tolerance and the C_s cost, $C_s = 47$ nF is chosen. Then, the preferred theoretical parameter set can be confirmed: $C_s = 47$ nF, $L_s = 380$ μH (leakage inductance from the primary side), $A_c = 33.8$ and N_{TR} is 4.05.

To allow enough transformer manufacturing margin from the productivity perspective and to make the C_p a standard value, N_{TR} is selected to be 4.42 (62 primary turns/14 secondary turns) in the real transformer design. This turns ratio together with the right current rating of Litz wire results in a leakage inductance of 360 μH .

When the integrated LCC transformer concept is selected, the parallel resonant capacitor can be placed across the secondary windings of the transformer (see C_{PS} in [Figure 23](#)). Then, this C_{PS} can be calculated as follows:

$$C_{PS} = \frac{C_s N_{TR}^2}{4A_c} \quad \text{Eq. 12}$$

Then, C_{PS} in this 100 W design is 6.8 nF.

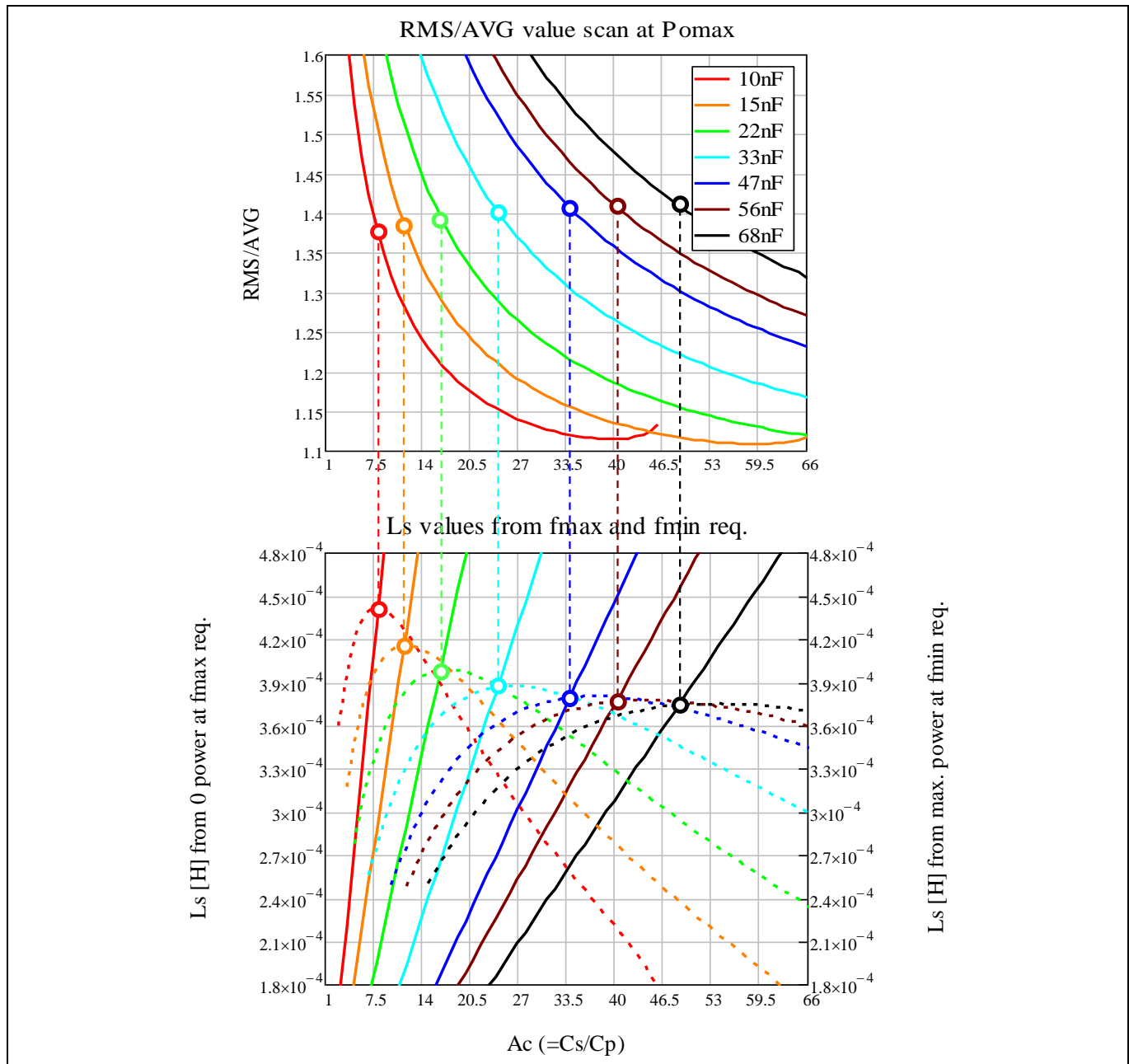


Figure 22 Use of two design charts combined to extract the optimal parameter set

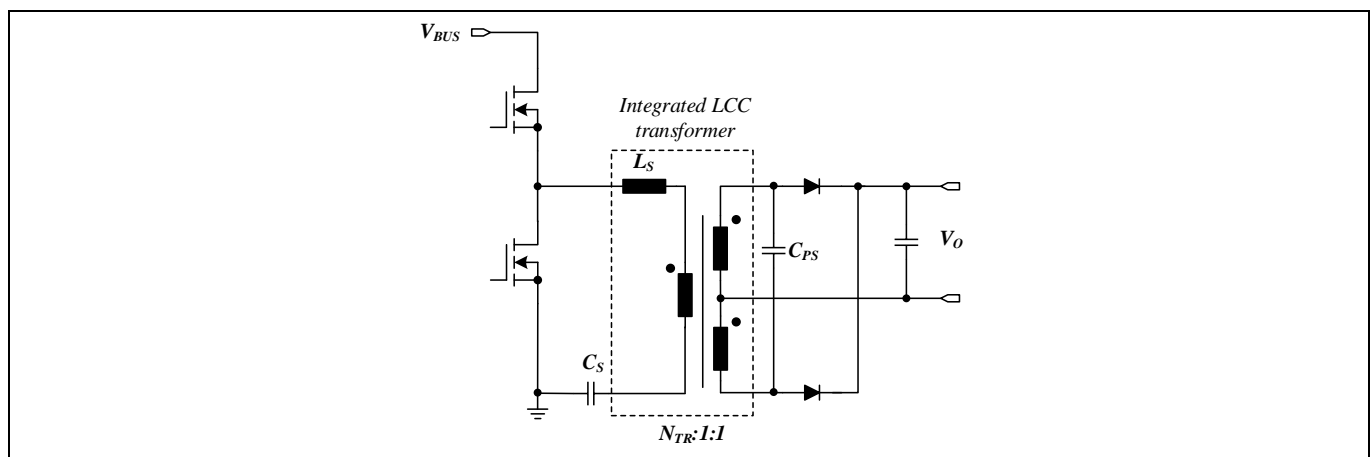


Figure 23 LCC with the parallel resonant capacitor placed on the transformer secondary side

4.4 Result validation

Designers can use the SPICE simulation to check the accuracy of selected parameter set. Compared with LLC, the operation of LCC is less sensitive to the parasitic capacitances on the secondary side, so the SPICE simulation is quite reliable as an approach to validating this LCC design tool.

This tool can plot the transformer current waveform with the selected parameter set. It can check whether the waveform has a preferred trapezoidal shape, and can be compared to the SPICE simulation to check how accurate the modeling is.

Figure 24 compares the waveforms from the LCC design tool, the SPICE simulation and the experimental demonstration board of the above-mentioned 100 W design. The SPICE simulation uses the theoretical parameters calculated from the LCC design tool. It can be seen that the LCC design tool is quite accurate.

Figure 24c shows the experimental waveforms of the hardware demonstration. The waveform is quite close to those from the design tool and the SPICE simulation, but the operating frequency is adapted to 185 kHz by the control loop in the demo board in order to reach 100 W, which is only 5 kHz more than the specified 180 kHz used in the design tool and the SPICE simulation.

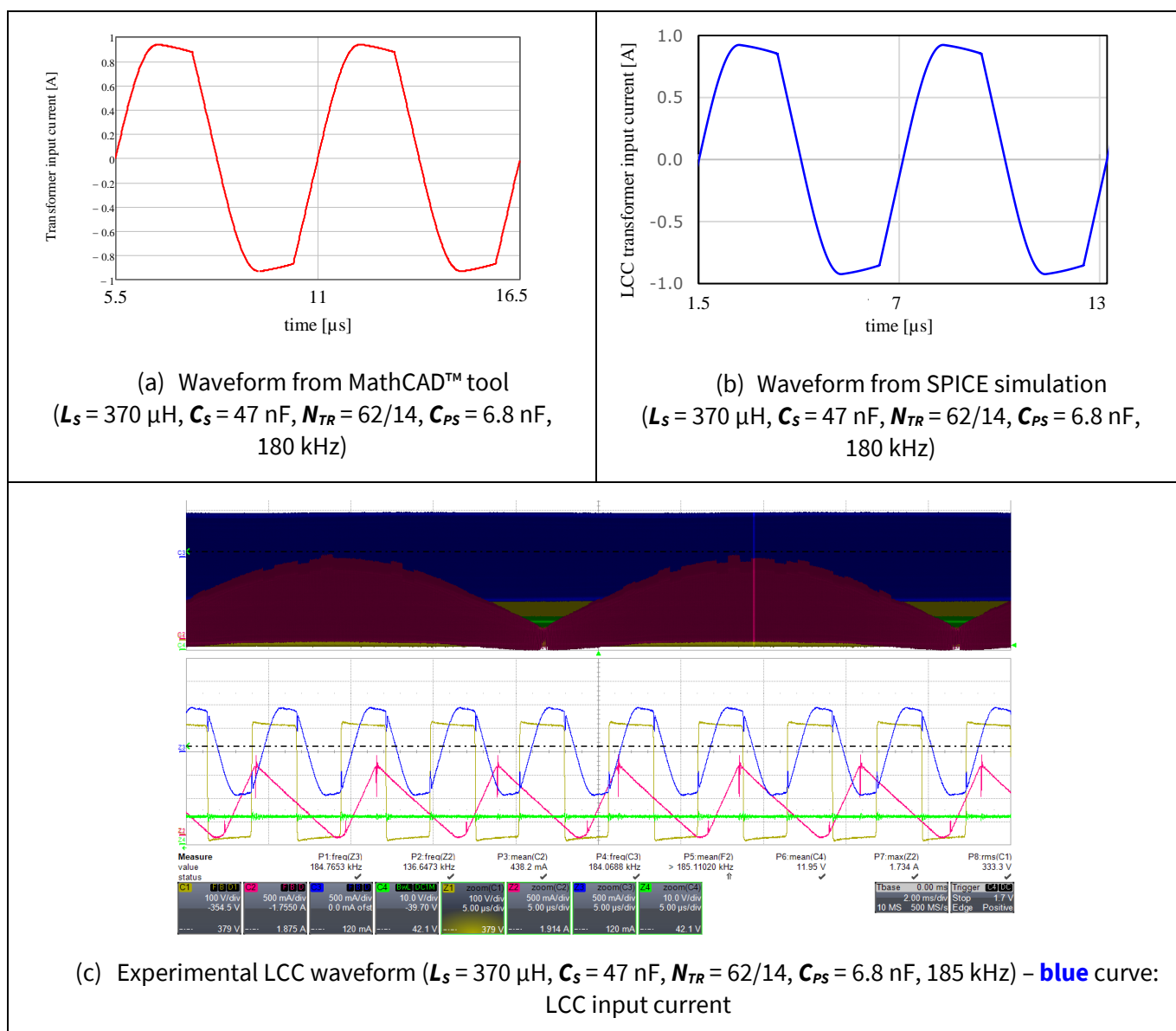


Figure 24 LCC input current waveforms at 100 W, 55 V LED from (a) MathCAD™ tool (b) SPICE simulation (c) experiments

Design tool for LCC with wide load range

In the experiment with the selected parameter set, the frequency reaching zero power at the minimum output voltage is 460 kHz, 10 kHz higher than the assumed maximum operating frequency. Other design examples given in the next chapter will again prove the accuracy of this LCC design tool.

4.5 Summary

An accurate and easy-to-use LCC design tool has been introduced. It can quickly calculate the four key parameters of the LCC resonant tank without iterations with the given specification. This tool can also indicate the relative efficiency of various parameter sets. How to use it and how to validate the result have also been described.

5 LCC design examples based on ICL5102

Three LCC reference boards have been built to demonstrate the superior performance of ICL5102/HV and the unique characteristics of the LCC topology. These boards and their key features are listed in [Table 3](#).

Table 3 Three LCC reference boards based on ICL5102 and their key features

LCC boards	Key features
100 W PFC + LCC (ICL5102)	- High frequency and integrated LCC transformer
	- Superior power quality, THD and harmonics
	- 1 percent dimming within output voltage 55~20 V
	- 93 percent system efficiency at 230 V _{AC} and full load
	- Low temperature of ICL5102 at 450 kHz operation
52 W PFC + LCC (ICL5102)	- Three fixed output current levels
	- High-frequency and integrated LCC transformer
	- Low-cost open-loop controlled LCC with narrow LED current spread across output voltage from 52 V to 20 V
	- 92.5 percent system efficiency at 230 V _{AC} and full load
150 W PFC + 800 V LCC (ICL5102HV)	- 800 V bus voltage
	- 1 percent dimming across output voltage from 48 V to 17 V

Before introducing the details of these three demonstration boards, the approach to setting the HB frequency range of the ICL5102 is described. This is not only essential to fulfill the specification of the frequency range in the steady-state, but is also critical to LCC or LLC performance at start-up.

5.1 Frequency set circuit of ICL5102

Designers always need to define the frequency range of LLC or LCC controlled by ICL5102. The RF and BM pins of ICL5102 are in charge of:

- the HB operating frequency range
- the frequency entering burst mode
- the frequency behavior at start-up

5.1.1 Frequency set in the steady-state

The RF pin is always sourced by a stiff voltage V_{RF} (= 2.5 V) inside the chip. In the steady-state, the current flowing out of the RF pin controls the HB frequency via a current controlled oscillator (COO). The factor is 400 kHz/mA. There is always a resistor connected from the RF pin to the BM pin. The BM pin is internally pulled down to 2.25 V in the steady-state by a controlled current sink, but it will be further pulled down by the external current sink (optocoupler output, for example) to adjust the switching frequency.

A general example of the external circuit of RF pin and BM pin is shown in [Figure 25](#). In the steady-state, the maximum frequency occurs when the optocoupler output is saturated (its saturation voltage $V_{FB.sat} \approx 0.1\sim0.25$ V, typ.), and the minimum frequency happens when the optocoupler output is floated; in other words, the optocoupler does not sink any current. The capacitor across the optocoupler's output is optional. It is normally placed to avoid noise pickup when the feedback track is long, and its value should not be too high to avoid unacceptably slowing down the control response (less than or equal to 2.2 nF is a proper range).

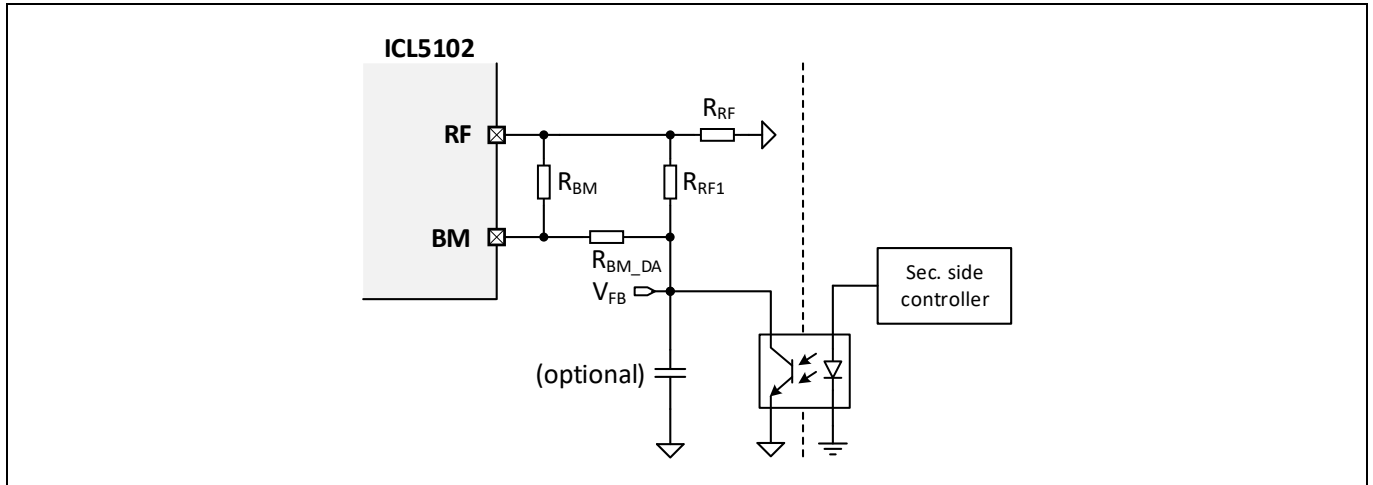


Figure 25 A general frequency set circuit around the RF pin and BM pin

Once the BM pin voltage $v(\text{BM})$ is smaller than $V_{\text{BM_ENTRY}}$ ($= 0.75 \text{ V}$) for longer than 10 ms, the ICL5102 enters burst mode. To disable burst mode, the ratio between $R_{\text{BM_DA}}$ and R_{BM} should follow [Eq. 13](#):

$$\frac{R_{\text{BM_DA}}}{R_{\text{BM}}} > \frac{V_{\text{BM_ENTRY}} - V_{\text{FB.sat.min}}}{V_{\text{RF}} - V_{\text{BM_ENTRY}}} \quad \text{Eq. 13}$$

When the minimum saturation voltage of the optocoupler $V_{\text{FB.sat.min}}$ is 0.1 V, this ratio is about 0.37. Here, leaving $R_{\text{BM_DA}}$ unmounted is the easiest way to disable burst mode.

To ensure that burst mode can be activated at light load, this ratio should follow:

$$\frac{R_{\text{BM_DA}}}{R_{\text{BM}}} < \frac{V_{\text{BM_ENTRY}} - V_{\text{FB.sat.max}}}{V_{\text{RF}} - V_{\text{BM_ENTRY}}} \quad \text{Eq. 14}$$

When the maximum saturation voltage of the optocoupler $V_{\text{FB.sat.max}}$ is 0.25 V, this ratio is about 0.28.

In a summary, the maximum operating frequency when burst mode is disabled can be calculated as:

$$f_{\text{max.BMdis}} = \frac{400 \text{ kHz}}{\text{mA}} \left(\frac{2.5\text{V}}{R_{\text{RF}}} + \frac{2.5\text{V} - V_{\text{FB.sat}}}{R_{\text{RF1}}} + \frac{2.5\text{V} - V_{\text{FB.sat}}}{R_{\text{BM}} + R_{\text{BM_DA}}} \right) \quad \text{Eq. 15}$$

The maximum operating frequency before entering burst mode when burst mode is enabled:

$$f_{\text{max.BMen}} = \frac{400 \text{ kHz}}{\text{mA}} \left(\frac{2.5\text{V}}{R_{\text{RF}}} + \frac{2.5\text{V} - 0.75\text{V}}{R_{\text{BM}}} + \frac{2.5\text{V} - V_{\text{FB}}}{R_{\text{RF1}}} \right) \quad \text{Eq. 16}$$

The maximum frequency when the BM pin voltage is 0.75 V and the optocoupler output is floating:

$$f_{\text{max}} = \frac{400 \text{ kHz}}{\text{mA}} \left(\frac{2.5\text{V}}{R_{\text{RF}}} + \frac{2.5\text{V} - 0.75\text{V}}{R_{\text{BM}}} + \frac{2.5\text{V} - 0.75\text{V}}{R_{\text{RF1}} + R_{\text{BM_DA}}} \right) \quad \text{Eq. 17}$$

This frequency is related to the start-up behavior.

The minimum frequency during steady-state:

$$f_{min} = \frac{400 \text{ kHz}}{mA} \left(\frac{2.5V}{R_{RF}} + \frac{2.5V - 2.25V}{R_{BM}} + \frac{2.5V - 2.25V}{R_{RF1} + R_{BM_DA}} \right)$$

Eq. 18

5.1.2 Frequency behavior in the start-up process

Soft start-up of the resonant HB topology helps smooth the output building up, reducing the voltage and current stress of the resonant tank and minimizing audio noise. To achieve a soft start-up, the frequency of the resonant HB topology ramps down from a high value before the control loop dominates. **Figure 26** illustrates a typical frequency behavior at soft start-up controlled by ICL5102.

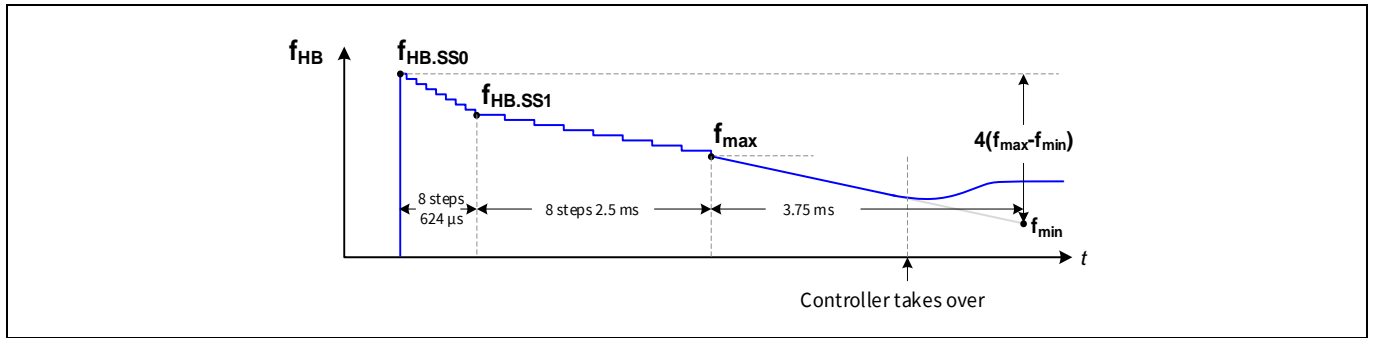


Figure 26 HB frequency behavior at soft start-up controlled by ICL5102/HV

The initial frequency of the soft start-up process is set to be $f_{HB.SS0}$ and it goes down in 624 μs by eight discrete steps to $f_{HB.SS1}$. Then, it further drops to f_{max} (defined in **Eq. 17**) in 2.5 ms by eight steps. In these two intervals, the frequency is regulated by an internal time-controlled oscillator (TCO), and the BM pin voltage is fixed at 0.75 V. After that, the $v(BM)$ ramps up from 0.75 V toward 2.25 V in 3.75 ms. If the optocoupler starts pulling current during this 3.75 ms, the control loop takes over the frequency control. If not, f_{min} (**Eq. 18**) is reached when $v(BM) = 2.25$ V. Here, $f_{HB.SS0}$ and $f_{HB.SS1}$ are defined as:

$$f_{HB.SS0} = 4(f_{max} - f_{min}) + f_{min}$$

Eq. 19

$$f_{HB.SS1} = 2.6(f_{max} - f_{min}) + f_{min}$$

Eq. 20

In the resonant HB controller where the switching duty cycle is fixed to be 50 percent, it is inevitable to have a number of initial switching cycles experiencing a kind of hard-switching (**Figure 27**), where the body diode of one MOSFET is in reverse recovery while the complementary MOSFET is switched on. A detailed description of this process can be found in **[10]**. The temporary shooting through induces a severe di/dt and dV/dt in the circuit that harms the system reliability. This phenomenon demands a MOSFET body diode with a very small reverse recovery charge. Here, Infineon's P7 series 600 V MOSFETs are perfect candidates. However, it is always advantageous to reduce the number of hard-switching events as much as possible.

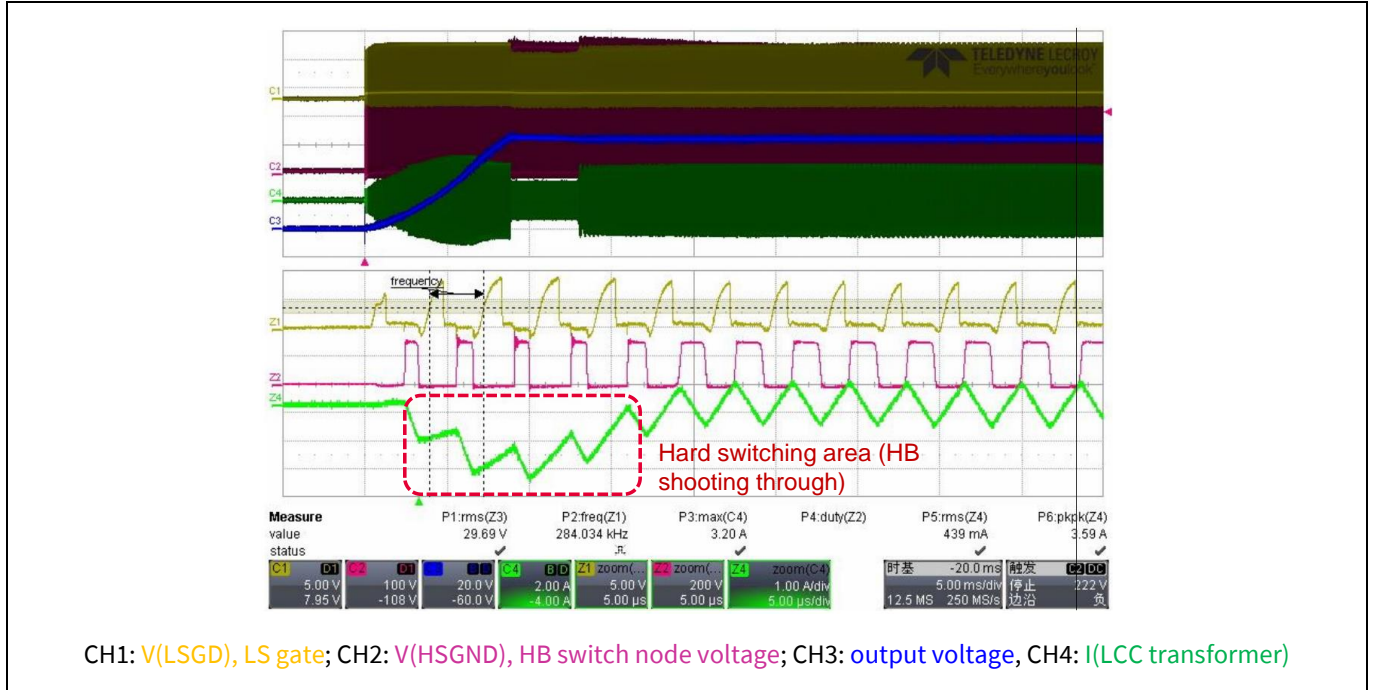


Figure 27 Typical start-up behavior of a resonant HB topology

As mentioned in [section 3.2.2](#), an efficient LCC requires a wide frequency to cover the wide load range. According to [Eq. 19](#), the initial frequency of the LCC soft start-up can be quite high if care is not taken. A solution is given below for the case that burst mode is disabled in non-standby mode. To disable burst mode, R_{BM_DA} can be simply left open and then the f_{HB_SS0} becomes:

$$f_{HB_SS0} = \frac{400 \text{ kHz}}{mA} \left(\frac{2.5V}{R_{RF}} + \frac{6.25V}{R_{BM}} \right) \quad \text{Eq. 21}$$

The maximum frequency during steady-state operation is:

$$f_{max.BMdis} = \frac{400 \text{ kHz}}{mA} \left(\frac{2.5V}{R_{RF}} + \frac{2.5V - V_{FB_sat}}{R_{RF1}} + \frac{2.5V - 2.25V}{R_{BM}} \right) \quad \text{Eq. 22}$$

One can adjust the values of R_{BM} and R_{RF1} to set the relation between f_{HB_SS0} and the maximum frequency at the minimum power $f_{max.BMdis}$. The rule of thumb here is to leave f_{HB_SS0} a little bit larger than $f_{max.BMdis}$. This guarantees a smooth output building up and limited hard-switching at start-up. Note that using splitting series resonant capacitors helps speed up the establishment of the tank voltage and current to reach the soft-switching state [\[11\]](#).

Below are examples of three LCC designs that have been developed based on ICL5102 and ICL5102HV.

5.2 A high-frequency LCC design example – 100 W

ICL5102/HV's coreless transformer-based HS driver is highly robust and efficient. It can operate up to 500 kHz in the steady-state with high bus voltage, and this 500 kHz is not a destructive limit from a loss perspective. A 100 W reference board [\[6\]](#) has been developed to not only demonstrate the high-frequency capability of the HB driver integrated in ICL5102/HV but also to show the possibility of an efficient, compact and integrated LCC transformer at high frequency.

5.2.1 System specification and LCC design inputs

The key system specifications of this board are shown in [Table 4](#). The main features are the universal mains input with the demanding power quality and 1 percent dimming with wide LED range (20~55 V).

Table 4 Key electrical specifications of the 100 W LCC demo for LED lighting applications

Item	Symbol	Min.	Typ.	Max.	Unit	Remarks
AC input voltage	$V_{in,ac}$	90	–	267	V_{RMS}	
Brown-out voltage	$V_{in,BO}$	–	83	–	V_{RMS}	Tested 50 Hz mains
Brown-in voltage	$V_{in,BI}$	–	90	–	V_{RMS}	Tested 50 Hz mains
Input frequency	f_{in}	47	–	63	Hz	
Efficiency	η	–	93 percent	–	–	100 percent load at 230 V_{RMS} , 50 Hz
Rated LED voltage	V_{LED}	20	–	55	V	
Full LED current	$I_{LED,max}$	–	1.82	–	A	
Min. LED current	$I_{LED,min}$	–	0.018	–	A	
Analog dimming voltage	V_{DIM}	0	–	10	V	
Total harmonic distortion	THD	–	–	10	%	More than 20 percent load at 267 V_{RMS} , 50 Hz
Power factor	PF	0.9	–	–		More than 30 percent load at 267 V_{RMS} , 50 Hz

[Table 5](#) summarizes the inputs to the LCC design tool. Here, high-frequency operation is required to realize an integrated LCC transformer concept with a desired EFD25.4/19/9 core set.

Table 5 LCC design tool inputs – 100 W LCC

LCC design specification	Symbol	value
Bus voltage	V_{BUS}	450 V
Max. output voltage	$V_{Omax.Pmax}$	55 V
Min. output voltage	V_{Omin}	22 V
Max. power	P_{Omax}	100 W
Min. load	P_{min}	1 W
Frequency at P_{Omax} and $V_{Omax.Pmax}$	$f_{Pmax.Omax}$	180 kHz
Frequency at 0 W and V_{Omin}	$f_{max.0W}$	450 kHz
Integrated LCC transformer core set		EFD25.4/19/9

5.2.2 Design and performance

The design process has already been given in [section 4.3.3](#). The final LCC resonant tank parameters are listed again below:

- $C_S = 47$ nF
- $L_S = 360$ μ H (using transformer leakage inductance)
- $C_P = 6.8$ nF
- N_{TR} is 4.42 (62 turns/14 turns)

Design of efficient LCC based on ICL5102/HV combo controller IC

Focusing on applications with wide output voltage and current range



LCC design examples based on ICL5102

High operating frequency demands less series resonant inductance at the same power, and at 180 kHz level we are able to utilize the leakage inductance of transformer core set EFD25.4/19/9 as the resonant inductance.

Figure 28 shows this 100 W board.

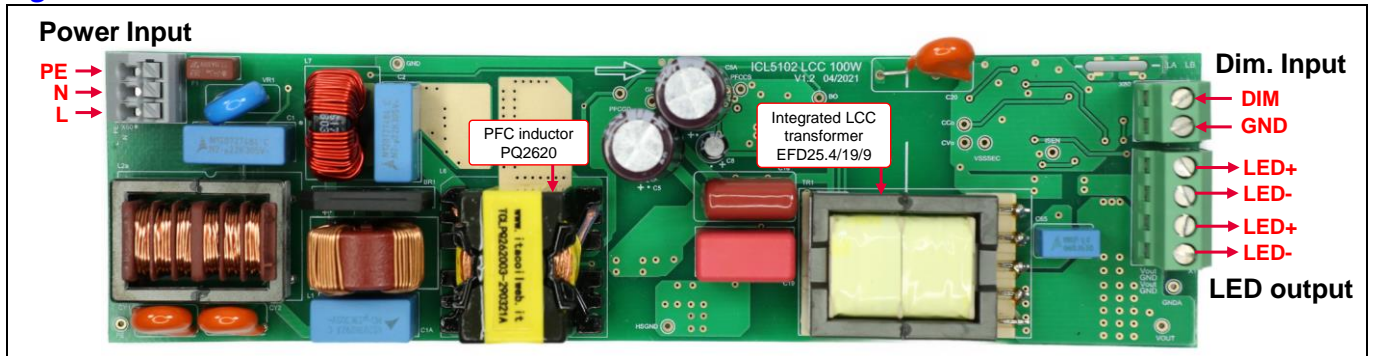


Figure 28 100 W PFC + LCC board

The system efficiency, power factor and THD information of this board are provided in **Figure 29**. Here is a summary of the results:

- The efficiency is 93 percent at 230 V_{AC} and 91.5 percent at 120 V_{AC}.
- Power factor greater than 0.9 at 267 V_{AC} above 30 percent load.
- THD less than 12 percent at 267 V_{AC} above 10 percent load.

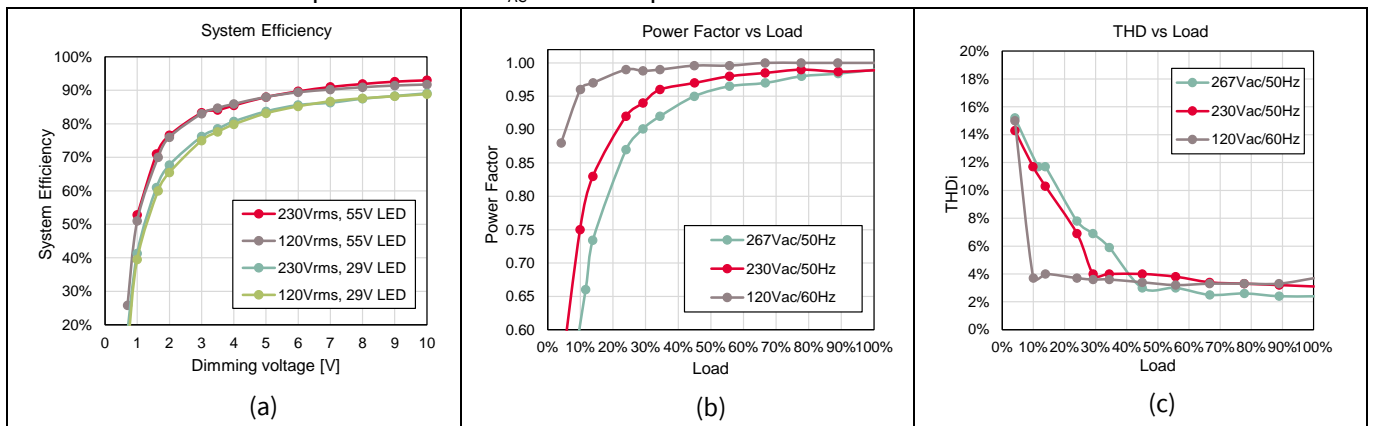


Figure 29 System performance of the 100 W demo (a) system efficiency, (b) power factor and (c) THD

Key PFC and LCC waveforms and an infrared thermal image are shown in **Figure 30**.

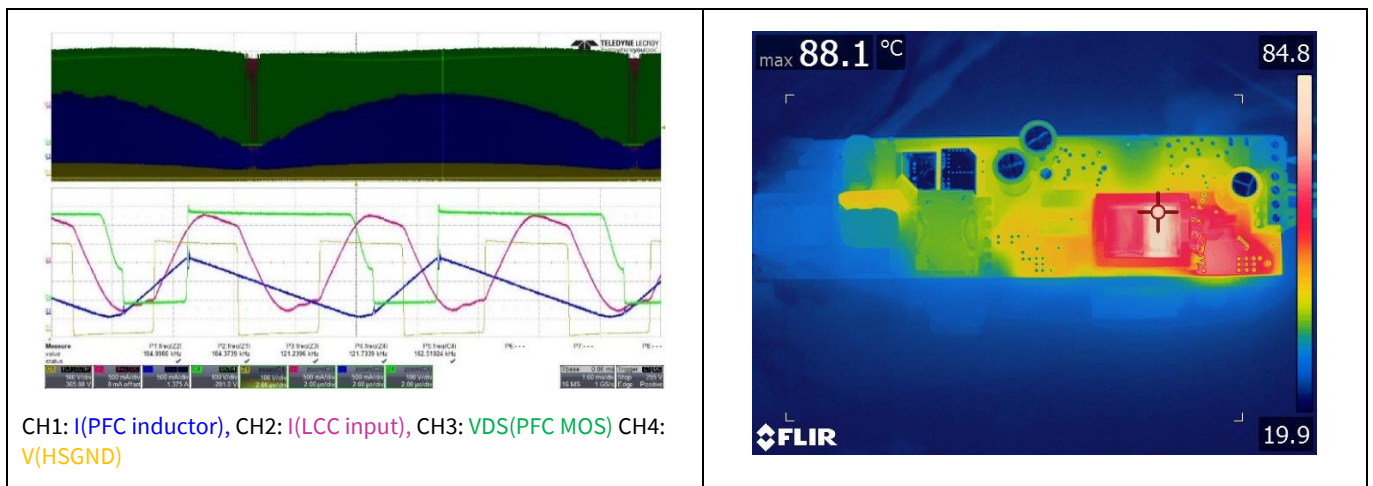


Figure 30 (a) Key PFC and LCC waveforms; (b) infrared thermal image (22°C room temperature) at full load

LCC design examples based on ICL5102

In the LCC design tool, 450 kHz is assumed as the maximum frequency to reach 0 W at 20 V output. Experiments on the final LCC transformer show 1 W output at 447 kHz. The accuracy of this tool is shown to be good. A thermal camera captures the ICL5102 temperature at such a high frequency but only 50°C, which proves ICL5102 is an excellent choice of high-frequency high-power-density converter design.

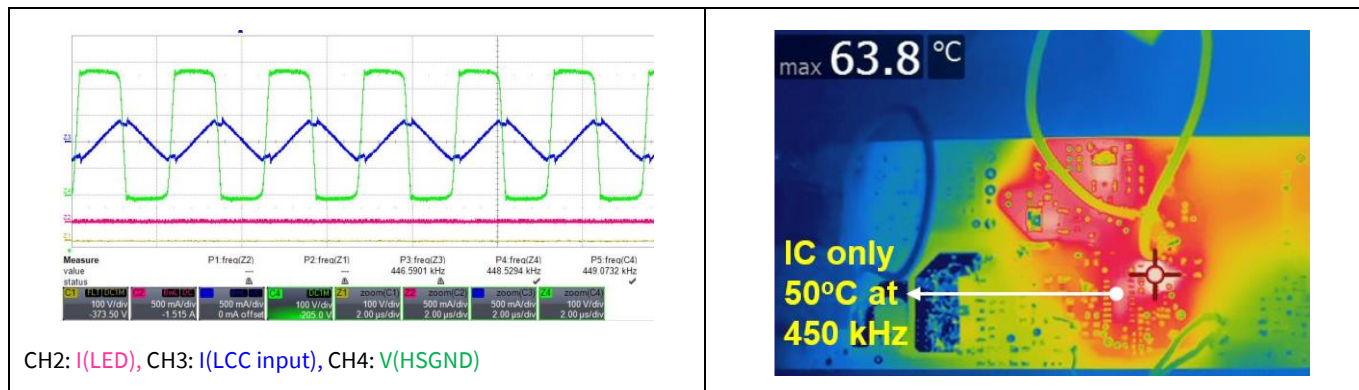


Figure 31 Performance at 447 kHz and 1 W: (a) waveforms at 1 W and 21 V LED (b) infrared thermal picture (22°C room temperature)

5.3 A low-cost open-loop controlled LCC design – 52 W

Non-dimmable LED lighting has a large market share. Some applications demand low cost as well as high light quality. Here, PFC + DC-DC stage can be considered as an interesting solution. Targeting this application, a 52 W high-frequency LCC with open-loop control has been developed [7] as the DC-DC stage. The open-loop control omits the expensive optocoupler and the negative feedback controller on the secondary side used in the closed-loop control, and the high-frequency operation enables the use of a compact integrated transformer. Here, the design difficulty is to constrain the LED current spread as the LED load voltage varies.

5.3.1 System specification and LCC design inputs

A 52 W demo has been designed (Figure 31). It has three discrete output current levels (1000 mA, 880 mA, 780 mA) in a wide range of LED voltage (20~52 V). Three output current settings can be changed by toggling a mechanical switch onboard. The key specifications of this 52 W LCC design are shown below:

Table 6 Key specification of the 52 W LCC demo

Parameters	Symbol	Min.	Typ.	Max.	Unit	Remarks
AC input voltage	$V_{in,ac}$	198	220~230	256	V_{RMS}	
Input frequency	f_{in}	47		63	Hz	
Total harmonic distortion	THD			10 percent	–	Full load range and input voltage range
Efficiency	η		92.5 percent		–	At the maximum load
Targeted LED voltage	V_{LED}	20		52	V DC	
LED current setting 1	$I_{LED,s1}$		1000		mA	$V_{LED} = 20 \sim 52 V$ -20°C ~ 100°C
Current spread at setting 1	$\Delta I_{LED,s1}$	± 10 percent				
LED current setting 2	$I_{LED,s2}$		880		mA	
Current spread at setting 2	$\Delta I_{LED,s2}$	± 10 percent				
LED current setting 3	$I_{LED,s3}$		780		mA	$V_{LED} = 26 \sim 52 V$

Parameters	Symbol	Min.	Typ.	Max.	Unit	Remarks
Current spread at setting 3	$\Delta I_{LED.S3}$	± 10 percent				-40°C ~ 125°C

Table 7 summarizes the inputs to the LCC design tool.

Table 7 LCC design tool input – 52 W

LCC design specification	Symbol	Value
Bus voltage	V_{BUS}	400 V
Max. output voltage	$V_{Omax.Pmax}$	52 V
Min. output voltage	V_{Omin}	20 V
Max. power at $V_{Omax.Pmax}$	P_{Omax}	52 W
Frequency at P_{Omax} and $V_{Omax.Pmax}$	$f_{Pmax.Omax}$	180 kHz
Frequency at 0 W and V_{Omin}	$f_{max.0W}$	750 kHz
Integrated transformer core set		EF25/13/11

Here, the frequency at zero power and the minimum output voltage ($f_{max.0W}$) are just virtual values to constrain the design boundary. A large gap between $f_{max.0W}$ and $f_{Pmax.Omax}$ is taken for a good LCC efficiency. However, the start-up frequency must be suppressed with the method introduced in [section 5.1.2](#).

5.3.2 Design and performance

The design charts from the LCC design tool are shown in [Figure 32](#). We have found that the leakage inductance of the preferred core set EF25/13/11 can give 450 μ H maximum leakage with the Litz wires that have the right current rating. Therefore, $C_s = 47$ nF is selected. The gap between $f_{max.0W}$ and $f_{Pmax.Omax}$ is so large that the **RMS/AVG** value is only 1.2. The resonant tank parameters are summarized below:

- $C_s = 47$ nF
- $L_s = 433$ μ H (leakage inductance of the final transformer)
- $C_{PS} = 1.5$ nF
- N_{TR} is 3.5 (84/24)

The system efficiency and key PFC and LCC waveforms are given in [Figure 33](#). The system efficiency is about 92.5 percent at 230 V_{AC} and the maximum load. More test data on this board can be found in [\[7\]](#).

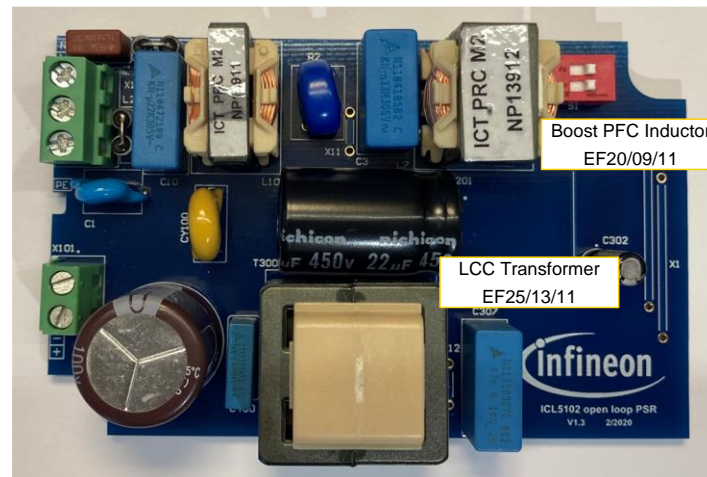


Figure 32 52 W board

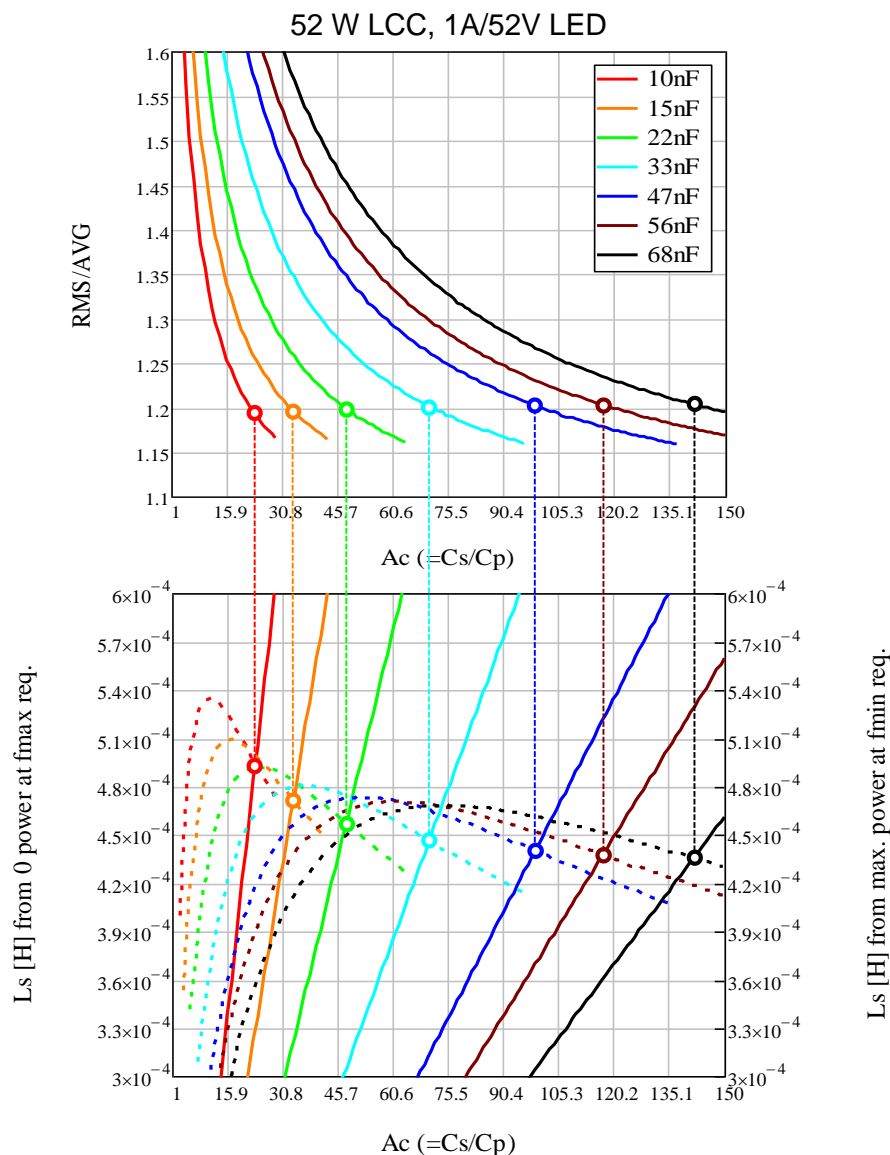


Figure 33 52 W LCC design charts – $C_s = 47$ nF is selected

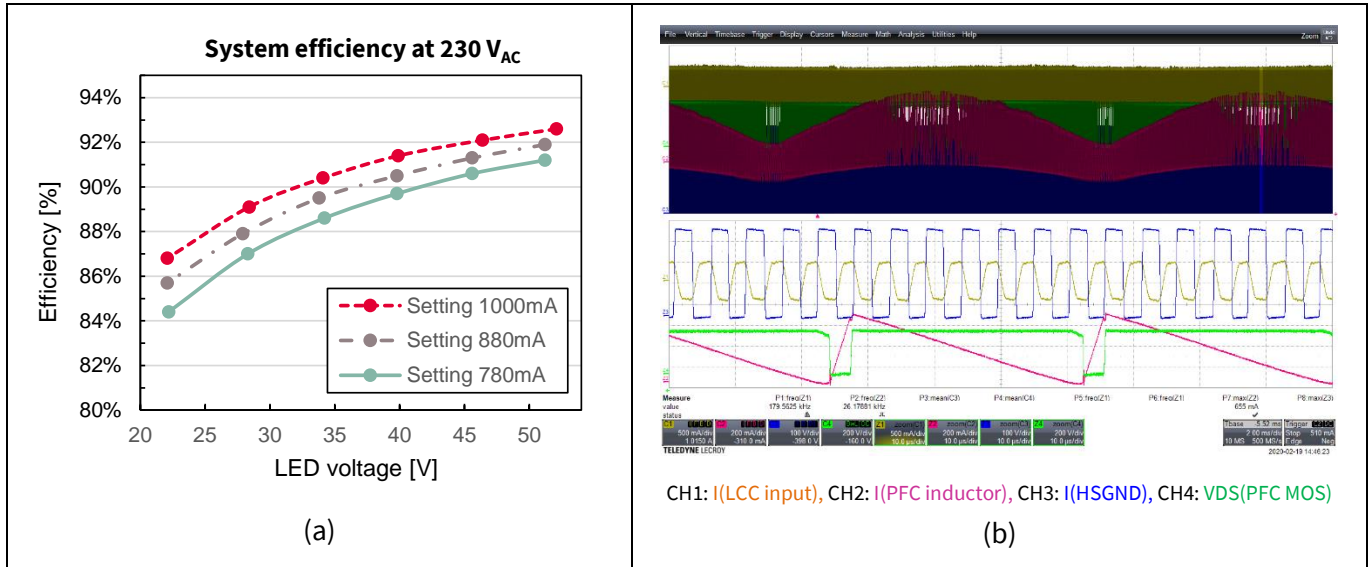


Figure 34 (a) System efficiency at 230 V_{AC}; (b) key waveforms of PFC and LCC at 52 W, 230 V_{AC}

The success of this open-loop LCC design depends on the LED current spread control. If the LCC frequency is fixed at a certain value, the output current will be output voltage dependent unless the frequency is on the CC point (see [Figure 8](#)). However, since three different current levels have been defined, working on the CC point is no longer possible. Therefore, the solution would be to introduce some output voltage dependency to the LCC frequency. The implemented circuit is shown in [Figure 35](#).

In this solution, R_{BM} , R_{RF0} , R_{RF1} and R_{RF2} are used to set the fundamental frequency f_{SET} . The mechanical switch toggles this fundamental frequency for three different output current settings. Using an auxiliary winding of the LCC transformer and a resistor network from this winding to the BM pin introduces an output voltage feed-forward to the frequency setting. The auxiliary winding must be coupled with the secondary side to get accurate output voltage information, and it has to be triple insulated. This auxiliary winding can be also used for output OVP. The detailed circuit design can be found in [\[7\]](#).

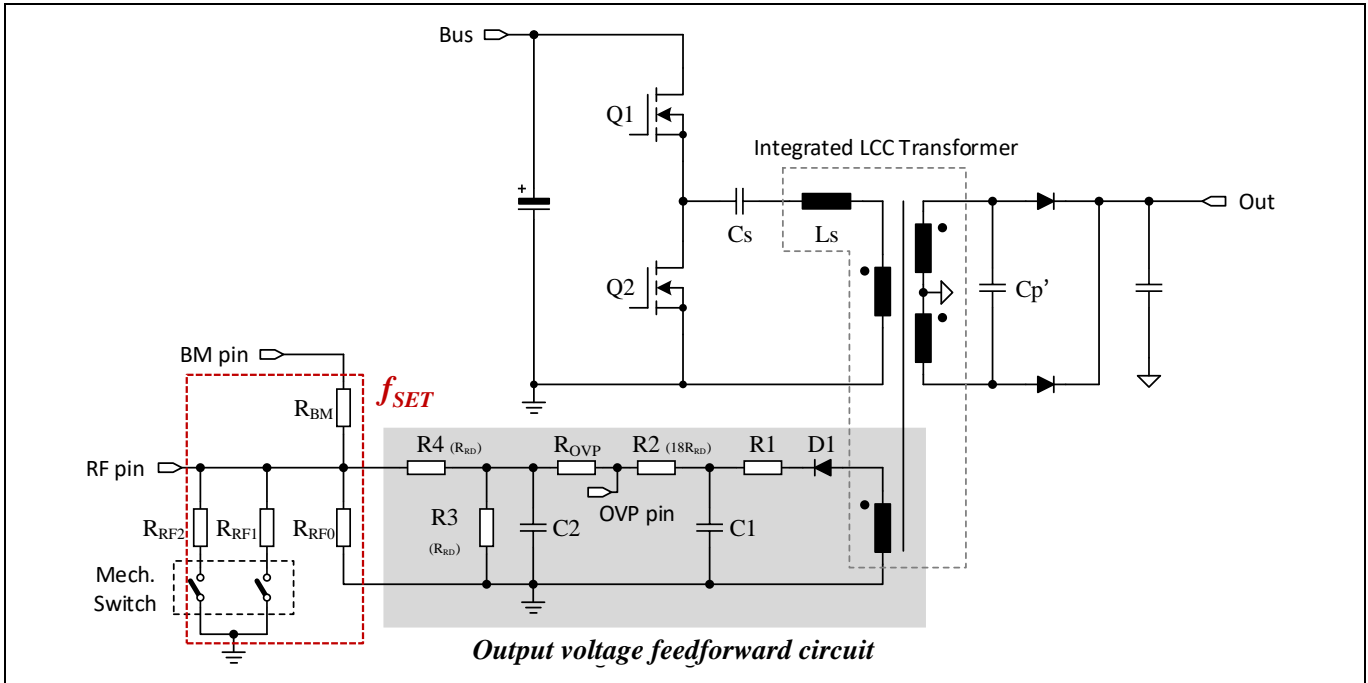


Figure 35 Output voltage feed-forward circuit to change the LCC frequency

With the designed feed-forward circuit, the LED current of this 52 W board is measured at different LED voltages and three current settings (see Figure 36). The current looks quite flat over the wide LED voltage range.

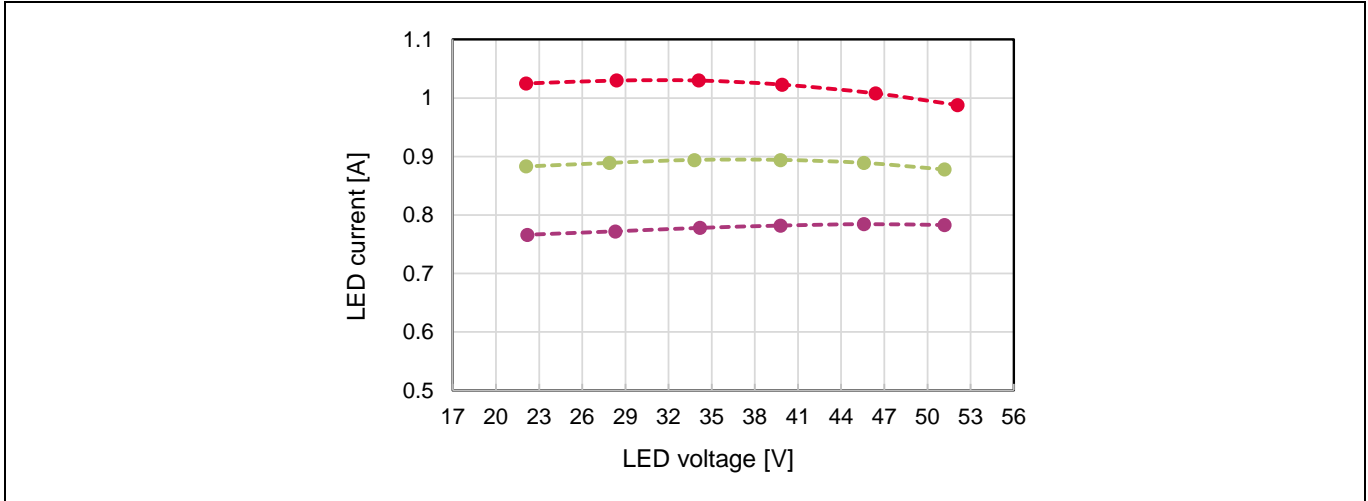


Figure 36 Measured LED current with the output voltage feed-forward network

However, to ensure the LED current spread fulfills the specification in mass production and over a wide temperature range, Monte Carlo analysis has been done in simulation with key component tolerances considered (see Table 8).

Table 8 Component tolerances considered in Monte Carlo analysis of LED current spread

Component	Tolerances	Specified standard deviation	Remarks
Series resonant capacitor (Cs)	±5 percent	3 σ	- Film capacitor

Component	Tolerances	Specified standard deviation	Remarks
Series resonant inductance (L_s)	± 5 percent, ± 7 percent, ± 10 percent	3σ	<ul style="list-style-type: none"> - 5 percent, standalone inductor - 10 percent, using leakage inductance of a transformer as the resonant inductor
Parallel resonant capacitor (C_{PS})	± 5 percent	3σ	- Film capacitor
Resistors in the feed-forward circuit	± 1 percent	3σ	- SMD resistor
Frequency as a function of RF pin current	± 5 percent	4σ	- For frequency of less than 210 kHz
	± 7 percent	4σ	- For frequency of less than 270 kHz and IC temperature greater than -20°C
Bus voltage	± 2 percent	3σ	- Considering the resistive divider and IC tolerances

LED current points in the Monte Carlo simulation are plotted in [Figure 37](#), where three leakage inductance (L_s) tolerances are specified in three graphs. Each graph contains 1600 simulation runs.

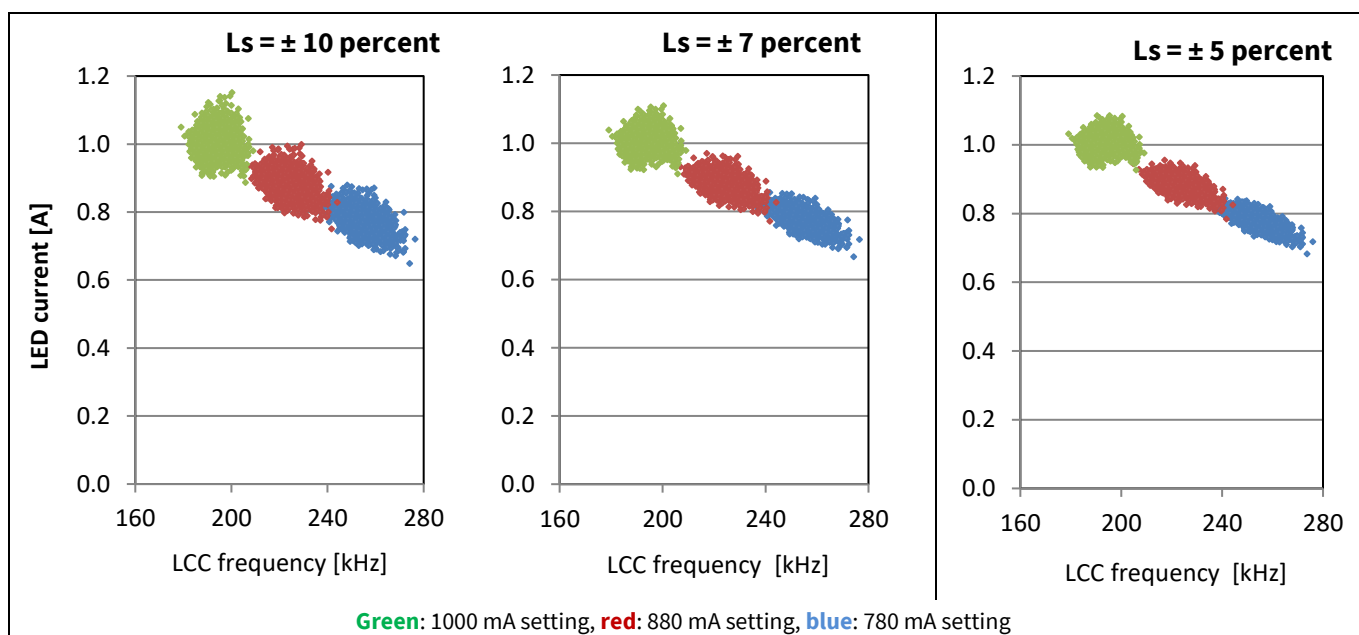


Figure 37 LED current points in 1600 Monte Carlo simulation runs (three leakage inductance tolerances are considered)

[Table 9](#) summarizes the results of LED current spread at three different L_s tolerance groups and with other specified component tolerances also given in [Table 8](#). Analysis shows that the leakage inductance L_s tolerance of less than ± 7 percent can fulfill the ± 10 percent LED current spread requirement.

Table 9 LED current spread analysis at different series inductance tolerance groups

Current settings	$L_s = \pm 10$ percent	$L_s = \pm 7$ percent	$L_s = \pm 5$ percent
1000 mA setting*	± 11.2 percent	± 8.7 percent	± 7.3 percent
880 mA setting	± 11.8 percent	± 9.4 percent	± 7.9 percent

LCC design examples based on ICL5102

Current settings	$L_s = \pm 10$ percent	$L_s = \pm 7$ percent	$L_s = \pm 5$ percent
780 mA setting**	± 13 percent	± 9.96 percent	± 9.2 percent

* IC frequency spread here is ± 5 percent because the switching frequencies are below 210 kHz

** In this setting, the specified LED voltage is down to 26 V

5.4 HV LCC – 150 W

ICL5102HV is the high-voltage (980 V max.) version of ICL5102. Its DSO19 package allows one empty pin position for sufficient creepage distance. A 150 W LCC reference board has been built [8] for industrial and horticultural lighting applications. For this HV case, a low LCC frequency (less than 150 kHz) is considered to enable easy passing of EMI.

5.4.1 System specification and performance

The key system specifications are given in Table 10. Main features are the high input voltage and 1 percent dimming without entering burst mode. The inputs to the LCC design tool are listed in Table 11. Note that a discrete resonant inductor is used. The maximum frequency at zero power is chosen to be 135 kHz, which is 15 kHz lower than 150 kHz, where the EMI limit drops sharply.

Table 10 Key specifications of the HV 150 W LCC demo

Item	Symbol	Min	Typ.	Max.	Unit	Remarks
AC input voltage	$V_{in,ac}$	277	380 to 480	528	V_{RMS}	
Input frequency	f_{in}	47		63	Hz	
Inrush current	$I_{in,pk}$			35	A_{pk}	
Total harmonic distortion	THD			10 percent	–	50 percent load, 380 V_{RMS}
				15 percent	–	50 percent load, 480 V_{RMS}
Efficiency	η	92 percent			–	100 percent load at 380 V_{RMS} and 480 V_{RMS}
Rated LED voltage	V_{LED}	17		48	V DC	
Full LED current	$I_{LED,full}$	2.97		3.03	A	
Min. LED current			0.03		mA	

Table 11 Key specifications of the HV 150 W LCC demo

LCC design specification	Symbol	value
Bus voltage	V_{BUS}	800 V
Max. output voltage	$V_{Omax,Pmax}$	48 V
Min. output voltage	V_{Omin}	17 V
Max. power	P_{Omax}	150 W
Min. power	P_{Omin}	1.5 W
Frequency at P_{Omax} and $V_{Omax,Pmax}$	$f_{Pmax,Omax}$	45 kHz
Frequency at 0 W and V_{Omin}	$f_{max,0W}$	135 kHz
Discrete resonant inductor		

5.4.2 Design and performance

The design charts from the LCC design tool are shown in **Figure 38**. $C_s = 47$ nF is selected as a balance between **RMS/AVG** value and the inductance value (cost-related). Smaller L_s implies a smaller external inductor.

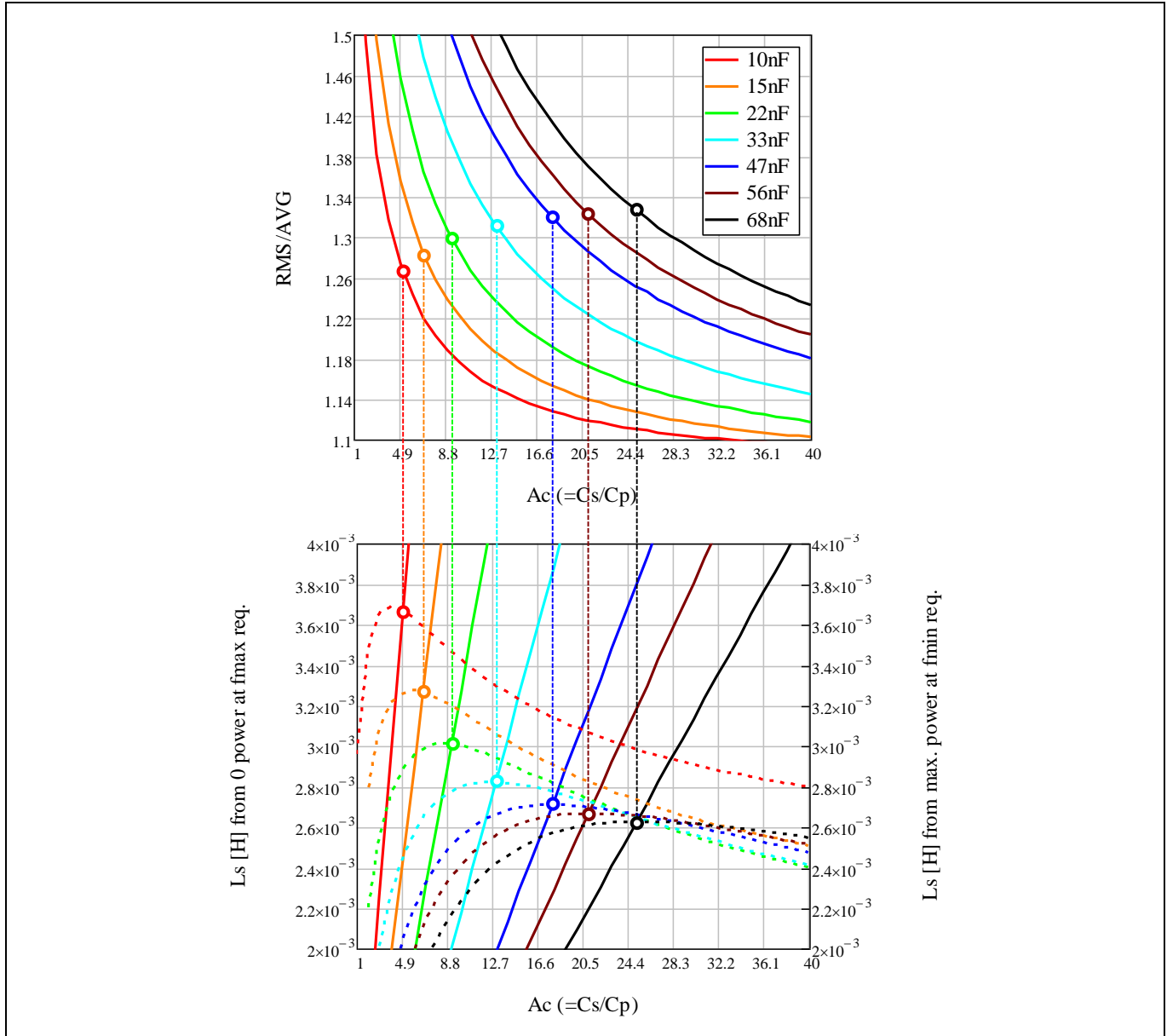


Figure 38 150 W LCC design chart

The selected resonant tank parameters are:

- $C_s = 47$ nF
- $L_s = 2700$ μ H
- $C_{PS} = 1.5$ nF
- N_{TR} is 7.14 (150 turns/21 turns)

In the end, the discrete resonant inductor has a value of 2.5 mH and the leakage inductance of the main transformer is 170 μ H.

The board picture is given in **Figure 39**. The system efficiency and key PFC and LCC waveforms are shown in **Figure 40**. More test results of this board can be found in [8].

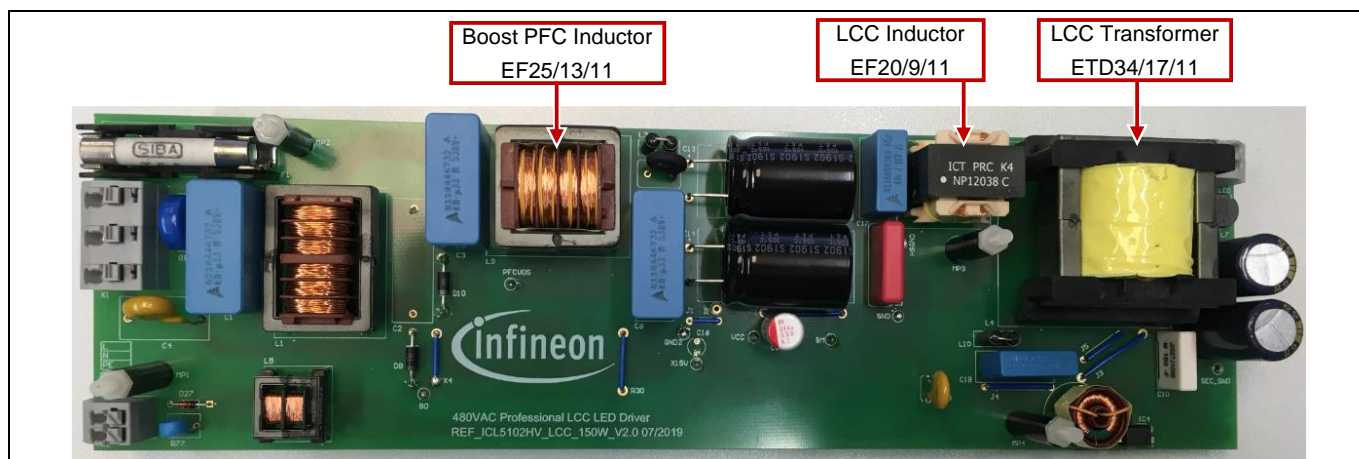


Figure 39 150 W LCC board (800 V bus voltage)

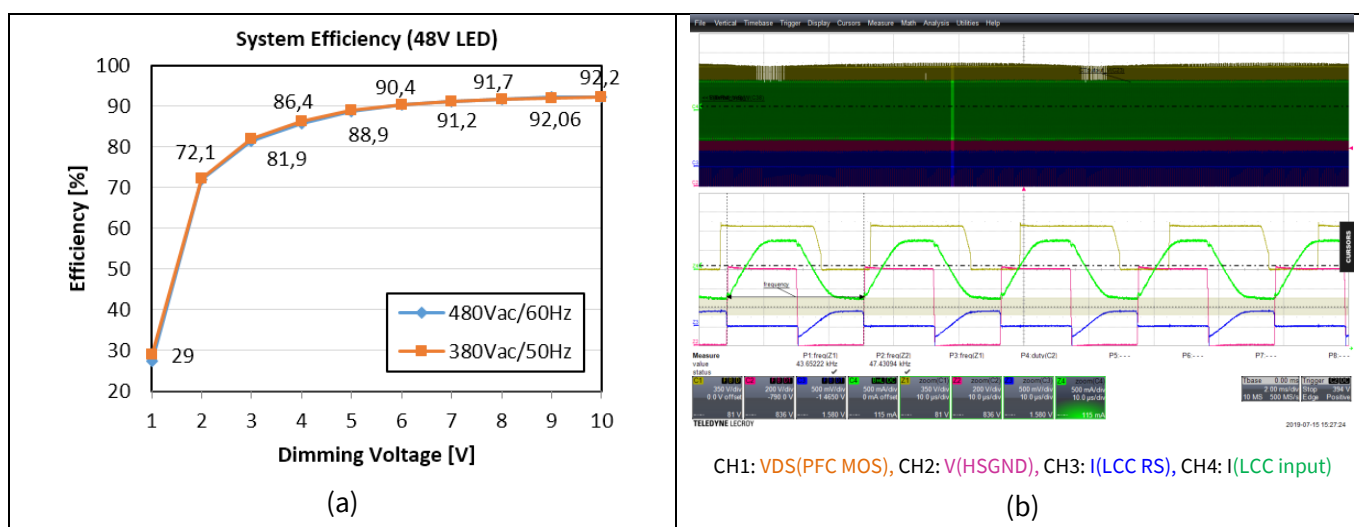


Figure 40 150 W LCC (a) system efficiency and (b) key waveforms of PFC and LCC at 480 V_{AC} and full load

5.5 Summary

How to set the HB operating frequency of ICL5102 has been introduced, as well as how to control the start-up frequency of an efficient LCC.

Three unique LCC designs utilizing the high-frequency capability of ICL5102 and the high-voltage feature of ICL5102HV have been presented.

1. The 100 W LCC design presents a high-frequency integrated LCC transformer. At the minimum load, 450 kHz and 450 V bus voltage, the ICL5102 temperature is only 50°C, which demonstrates the efficiency of the coreless transformer-based HB driver at high frequency.
2. The 52 W design, like the 100 W design, also implements a high-frequency integrated LCC transformer. The key feature is to tightly control the LED current spread in an open-loop control scheme.
3. The 150 W LCC design uses ICL5102HV to handle 800 V bus voltage. This 980 V HV PFC + LLC/LCC combo controller is unique on the IC market, and it provides greatly reduced system cost for HV power supply applications such as industrial SMPS and horticultural lighting.

In summary, ICL5102HV provides great value for applications requiring low system cost, high power density and high voltage.

6 References

- [1] R. Steigerwald, "A comparison of half-bridge resonant converter topologies", *IEEE Trans. Power Electron.*, vol. 3, pp. 174–182, Mar. 1988.
- [2] Sam Abdel-Rahman, Infineon Application Note, "Resonant LLC Converter: Operation and Design", https://www.infineon.com/dgdl/Application_Note_Resonant+LLC+Converter+Operation+and+Design_Infineon.pdf?fileId=db3a30433a047ba0013a4a60e3be64a1
- [3] C. C. Hua, Y. H. Fang and C. W. Lin, "LLC resonant converter for electric vehicle battery chargers", *IET Power Electron.*, vol. 9, no. 12, pp. 2369–2376, Oct. 2016.
- [4] R. Nielsen, "LLC and LCC resonance converters, properties, analysis control", http://www.runonielsen.dk/LLC_LCC.pdf
- [5] A. Pawellek, A. Bucher and T. Duerbaum, "Resonant LCC converter for low-profile applications", *MELECON 2010–2010 15th IEEE Mediterranean Electrotechnical Conference*, pp. 1309–1314, 2010.
- [6] Infineon Engineer Report, "100 W PFC + LCC LED driver design based on ICL5102 – 1 percent dimming with a compact LCC transformer operating with 180~450 kHz"
- [7] Infineon Engineer Report, "52 W low-cost two-stage LED driver based on ICL5102 – a PFC + open-loop LCC design with tight LED current spread"
- [8] Infineon Engineer Report, "150 W LCC LED driver demonstration with ICL5102HV – a 980 V combo PFC + half-bridge resonant controller"
- [9] Infineon Engineer Report, "130 W PFC + LLC LED driver design based on ICL5102 – 1 percent dimming with wide LED voltage and an integrated LLC transformer"
- [10] Infineon Application Note, "CoolMOS™ – primary-side MOSFET selection for LLC topology"
- [11] Infineon Design Guide, "Design of a 600 W HB LLC converter using 600 V CoolMOS™ P6"

Revision history

Revision history

Document version	Date of release	Description of changes
V 1.0	2021-09-13	First release

Trademarks

All referenced product or service names and trademarks are the property of their respective owners.

Edition 2021-09-13

Published by

Infineon Technologies AG

81726 Munich, Germany

© 2021 Infineon Technologies AG.

All Rights Reserved.

Do you have a question about this document?

Email: erratum@infineon.com

Document reference

DG_2104_PL39_2105_141034

IMPORTANT NOTICE

The information contained in this application note is given as a hint for the implementation of the product only and shall in no event be regarded as a description or warranty of a certain functionality, condition or quality of the product. Before implementation of the product, the recipient of this application note must verify any function and other technical information given herein in the real application. Infineon Technologies hereby disclaims any and all warranties and liabilities of any kind (including without limitation warranties of non-infringement of intellectual property rights of any third party) with respect to any and all information given in this application note.

The data contained in this document is exclusively intended for technically trained staff. It is the responsibility of customer's technical departments to evaluate the suitability of the product for the intended application and the completeness of the product information given in this document with respect to such application.

For further information on the product, technology, delivery terms and conditions and prices please contact your nearest Infineon Technologies office (www.infineon.com).

WARNINGS

Due to technical requirements products may contain dangerous substances. For information on the types in question please contact your nearest Infineon Technologies office.

Except as otherwise explicitly approved by Infineon Technologies in a written document signed by authorized representatives of Infineon Technologies, Infineon Technologies' products may not be used in any applications where a failure of the product or any consequences of the use thereof can reasonably be expected to result in personal injury.